



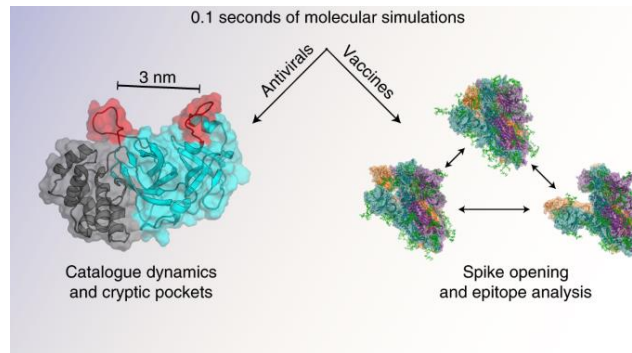
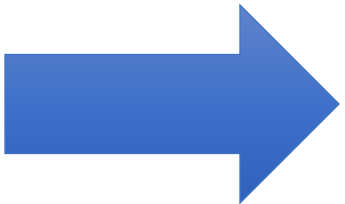
Duke Quantum Center

Duke
PRATT SCHOOL OF
ENGINEERING

Spin-Boson Dynamics in Trapped Ions

Ken Brown
Duke University

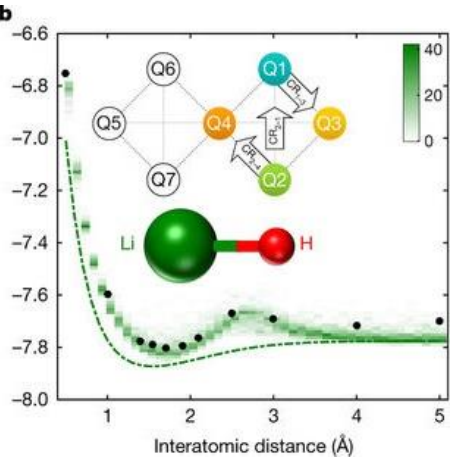
Computers have transformed chemistry



but

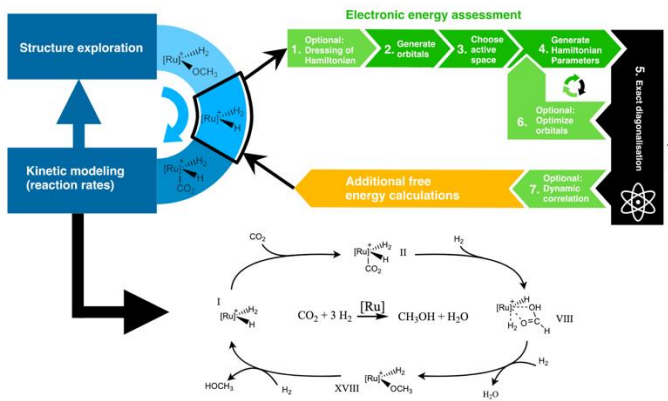


Electronic energy of LiH and BH^+
J. Chem. Phys. (1957)



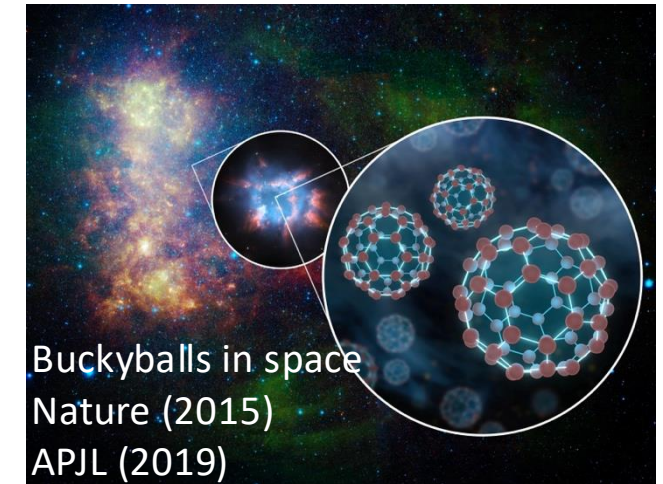
Electronic energy of LiH
Nature (2017)

Exa-scale SARS-CoV-2
Nat. Chem. (2021)



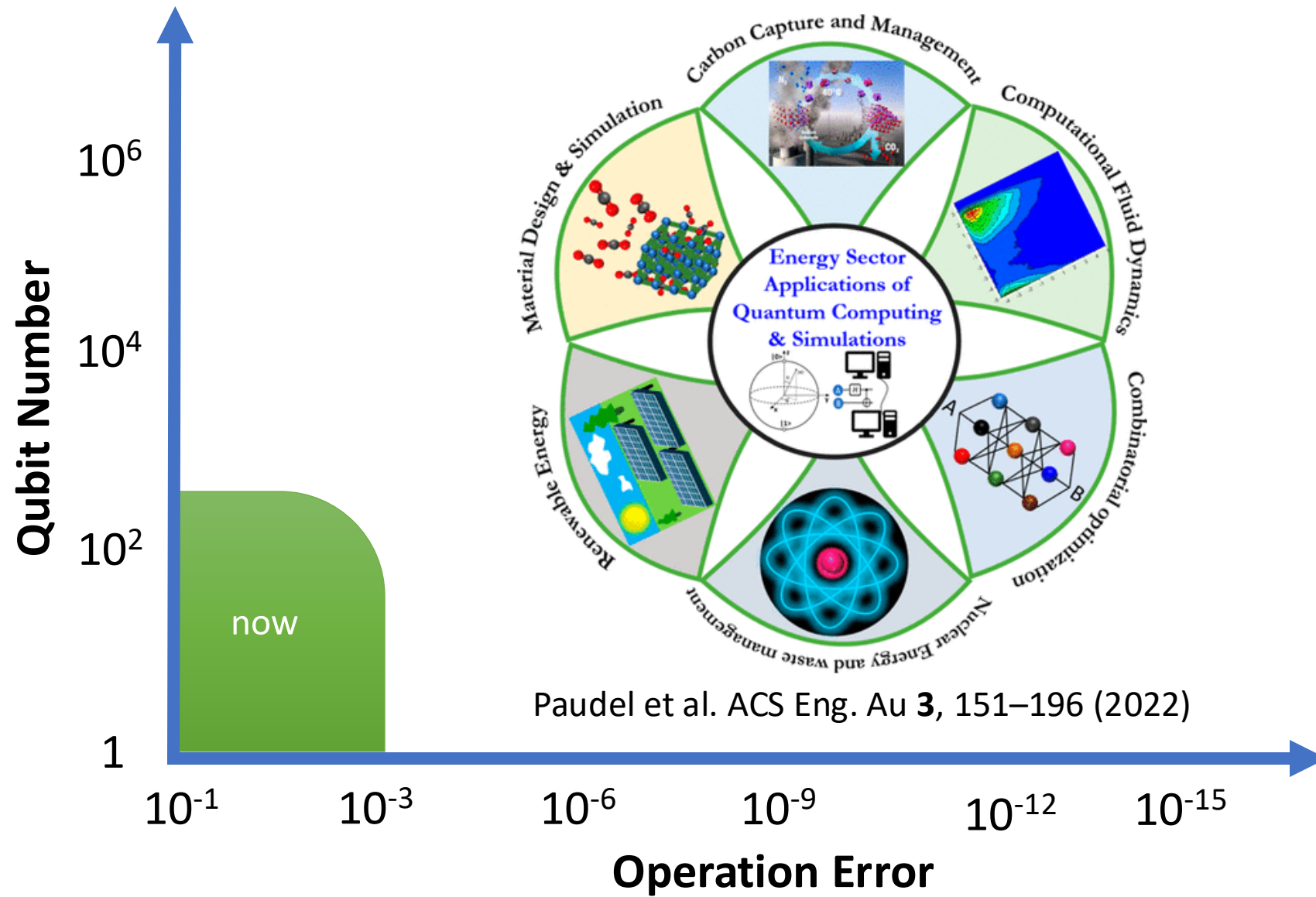
Quantum computing for catalysis
Phys. Rev. Res. (2022)

Benzene (C_6H_6) challenge
J. Phys. Chem. Lett. (2020)



Buckyballs in space
Nature (2015)
APJL (2019)

Where is my QPU?

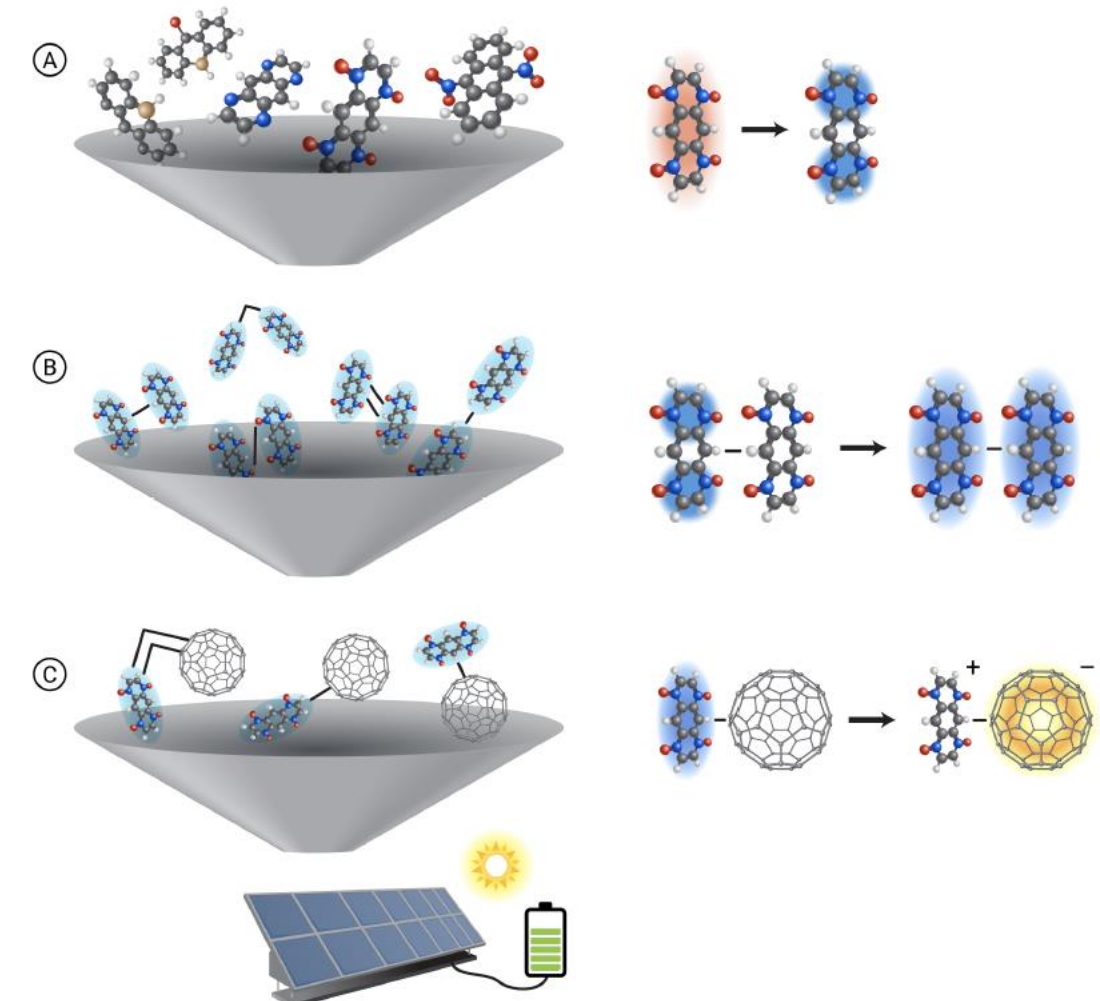


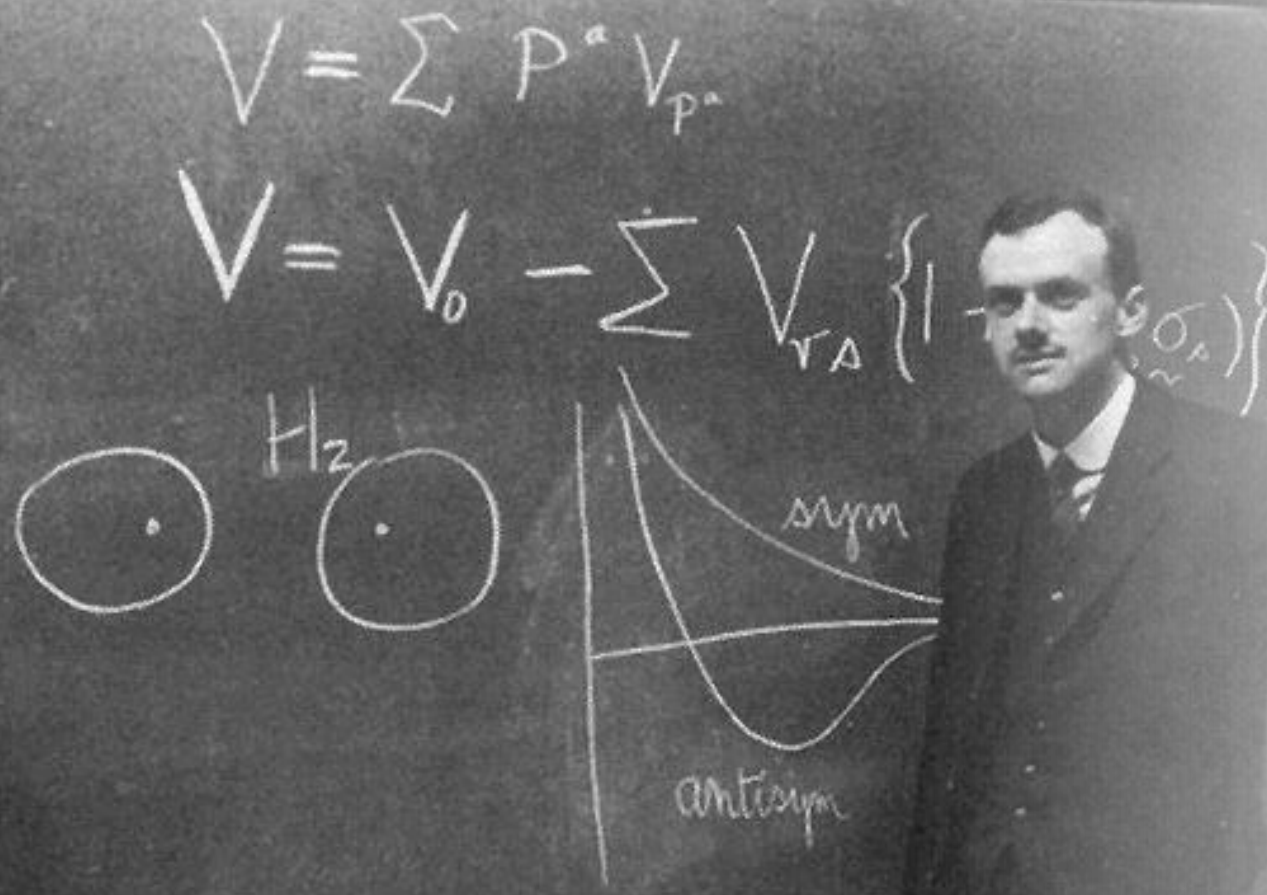
Solar cell optimization depends on vibronic dynamics

System	# Qubits	# Toffoli Gates	Parameters
(NO) ₄ -Anth [60]	148	8.9×10^8	$N = 5, M = 19, K = 16,$ $t = 100\text{fs}, \epsilon = 10\%$
	154	2.9×10^9	$N = 5, M = 19, K = 16,$ $t = 100\text{fs}, \epsilon = 1\%$
(NO) ₄ -Anth Dimer [129]	160	1.8×10^9	$N = 6, M = 21, K = 16,$ $t = 100\text{fs}, \epsilon = 1\%$
	164	2.0×10^{10}	$N = 6, M = 21, K = 16,$ $t = 500\text{fs}, \epsilon = 1\%$
Anth/C ₆₀ [63]	117	1.5×10^7	$N = 4, M = 11, K = 16,$ $t = 100\text{fs}, \epsilon = 1\%$
	1065	2.7×10^9	$N = 4, M = 246, K = 16,$ $t = 100\text{fs}, \epsilon = 1\%$

Quantum Algorithm for Vibronic Dynamics:
Case Study on Singlet Fission Solar Cell Design
D. Motlagh arXiv:2411.13669

Cost is driven by mapping bosons to qubits





- The underlying physical laws necessary for the mathematical theory of a large part of physics and the whole of chemistry are thus completely known, and the difficulty is only that the exact application of these laws leads to equations much too complicated to be soluble.
- P.A.M. Dirac, Proc. R. Soc. A **123**, 714 (1929)

Molecular Hamiltonian

$$\hat{H} = - \sum_A^{\text{nuc}} \frac{\hbar^2}{2M_A} \nabla_A^2 - \frac{\hbar^2}{2m} \sum_i^{\text{elec}} \nabla_i^2 - \sum_A^{\text{nuc}} \sum_i^{\text{elec}} \frac{Z_A e^2}{4\pi\epsilon_0 r_{Ai}} + \sum_{A>B}^{\text{nuc}} \frac{Z_A Z_B e^2}{4\pi\epsilon_0 R_{AB}} + \sum_{i>j}^{\text{elec}} \frac{e^2}{4\pi\epsilon_0 r_{ij}}$$

Nuclei Kinetic Energy

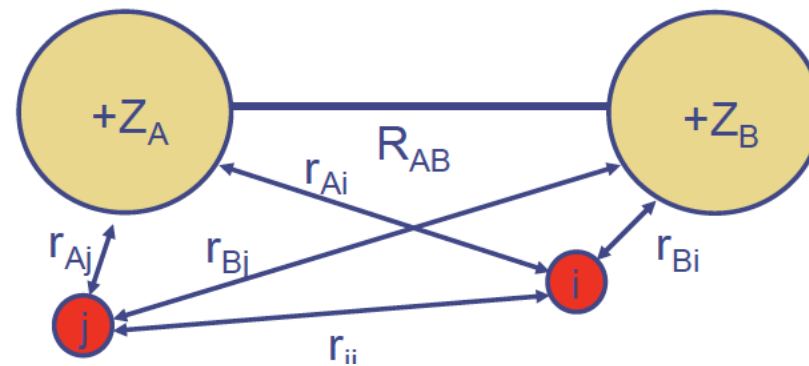
Nuclei-Electron Attraction

Electron-Electron Repulsion

$$\hat{H} = \hat{T}_N(\mathbf{R}) + \hat{T}_e(\mathbf{r}) + V_{eN}(\mathbf{r}, \mathbf{R}) + V_{NN}(\mathbf{R}) + V_{ee}(\mathbf{r})$$

Electron Kinetic Energy

Nuclei-Nuclei Repulsion



Born-Oppenheimer Approximation

$$\Psi(\mathbf{r}, \mathbf{R}) = \sum_k \Psi_k(\mathbf{r}; \mathbf{R}) \chi_k(\mathbf{R})$$

k electronic nuclear

Separate variables based on $M_N/m_e > 1$

Electronic wavefunction for fixed nuclei

$$\hat{H}_{el} = \hat{T}_e(\mathbf{r}) + V_{eN}(\mathbf{r}; \mathbf{R}) + V_{NN}(\mathbf{R}) + V_{ee}(\mathbf{r})$$

$$\hat{H}_{el}(\mathbf{r}; \mathbf{R}) \Psi(\mathbf{r}; \mathbf{R}) = E_{el}(\mathbf{R}) \Psi(\mathbf{r}; \mathbf{R})$$

Nuclei wavefunction based on distinct electronic states

$$[\hat{T}_N(\mathbf{R}) + T''_{kk}(\mathbf{R}) + E_{el}(\mathbf{R})] \chi_k(\mathbf{R}) = E \chi_k(\mathbf{R})$$

Kinetic

Potential

Electronic Structure Problem

$$\hat{H}_{el} = \hat{T}_e(\mathbf{r}) + V_{eN}(\mathbf{r}; \mathbf{R}) + V_{NN}(\mathbf{R}) + V_{ee}(\mathbf{r})$$



Second quantize

$$\hat{H}_e = \sum_{pq} h_{pq} \hat{a}_p^\dagger \hat{a}_q + \frac{1}{2} \sum_{pqrs} g_{pqrs} \hat{a}_p^\dagger \hat{a}_q^\dagger \hat{a}_s \hat{a}_r,$$



Map to qubits

Jordan-Wigner, Bravyi-Kitaev,
Superfast, etc.

$$\hat{H}_{el} = \sum_j P_j$$

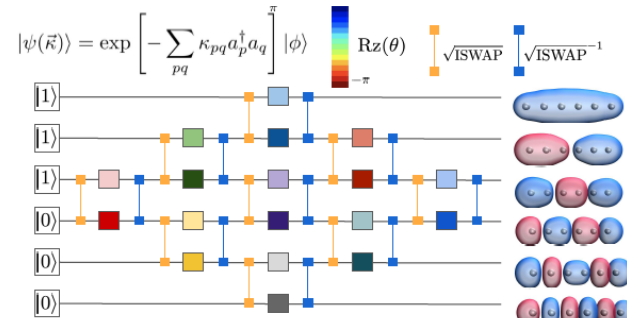
Phase Estimation

Abrams & Lloyd, PRL (1999)

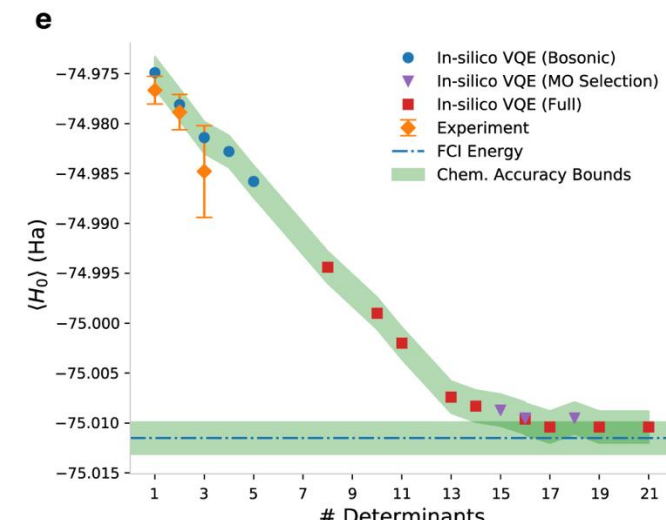
Aspuru-Guzik, Dutoi, Love & Head-Gordon Science (2005)

VQE

Peruzzo et al. Nat. Commun. (2014)



Arute et al. Science (2020)

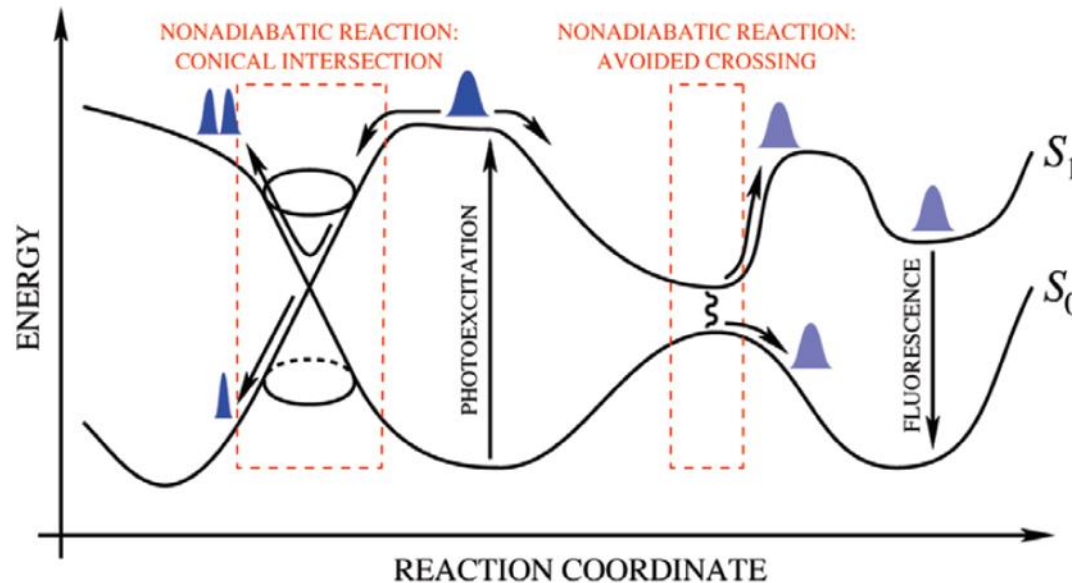


Nam et al. npj Quantum Information (2020)

Conical intersections and quantum simulation

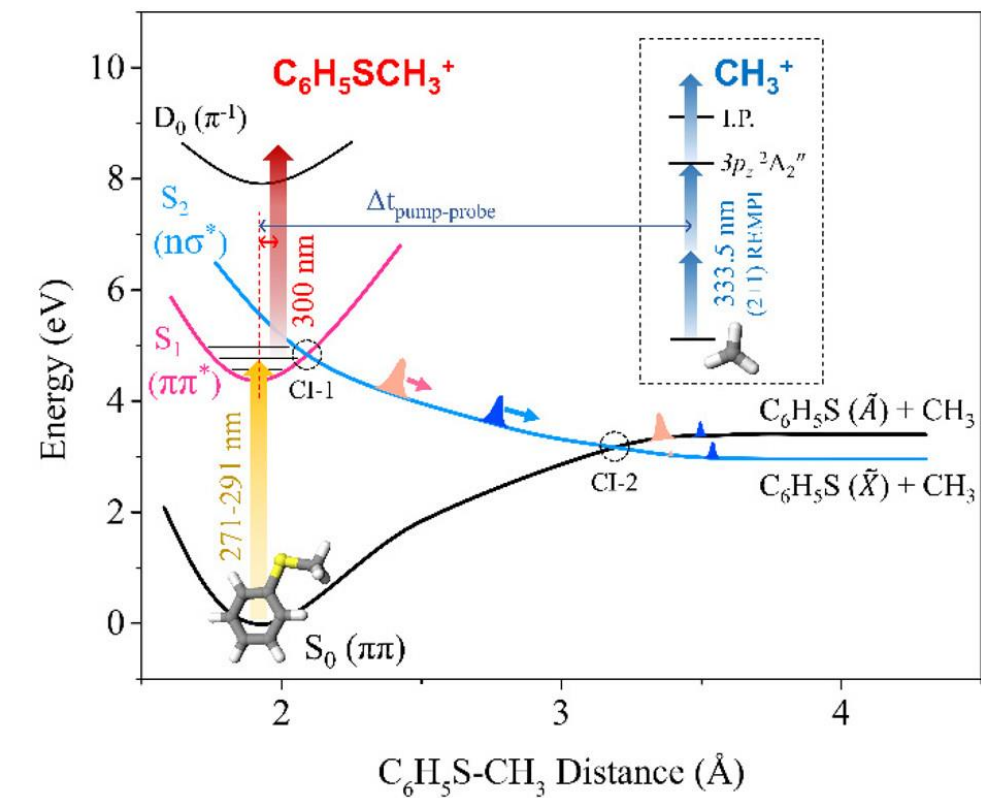
Conical intersections are ubiquitous in photochemistry.

Quantum simulation allows us to probe quantum effects that may be inaccessible to pump-probe spectroscopy



Photoexcited Vibrational Dynamics in Vicinity of Conical Intersections

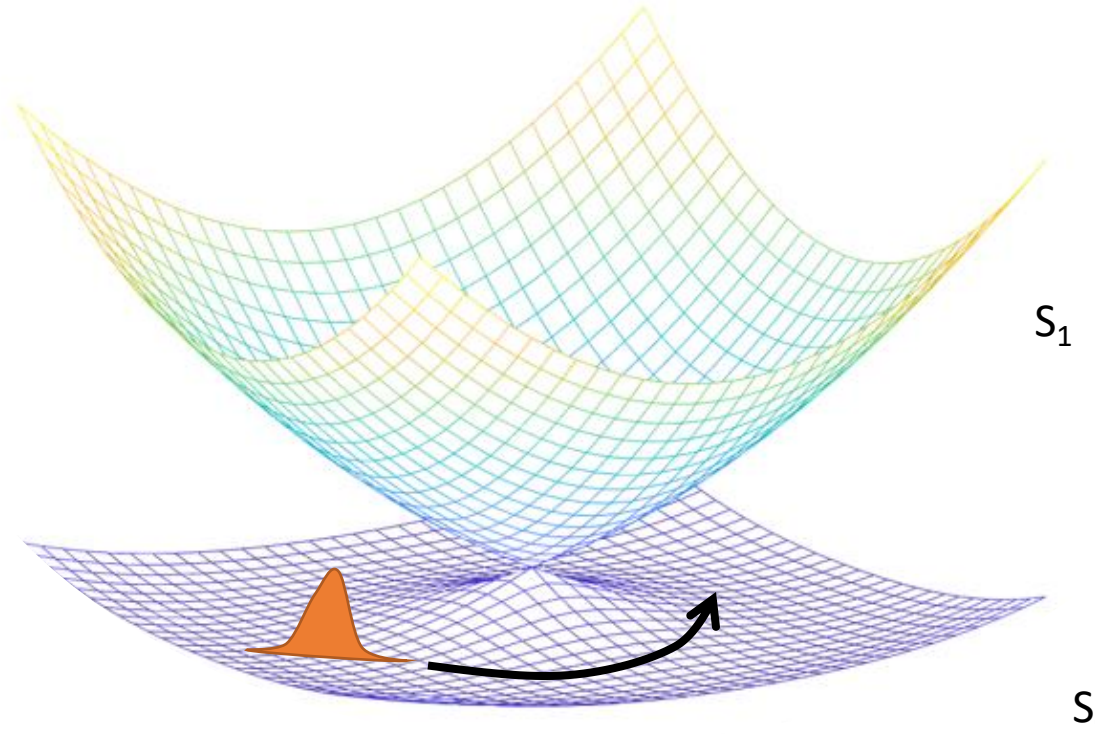
A. Piryatinski, S. Tretiak, M. Stepanov, and V. Chernyak, LALP-06-100 (2006)



Real-Time Observation of Nonadiabatic Bifurcation Dynamics at a Conical Intersection

K.C. Woo, D.H. Kang, and S.K. Kim JACS **139**, 17152 (2017)

Geometric phase on the ground state



Quantum mechanics predicts a geometric phase on the ground state potential

Femtosecond molecule

TIME-RESOLVED OPTICAL TESTS FOR ELECTRONIC GEOMETRIC PHASE DEVELOPMENT

JEFFREY A. CINA* and TIMOTHY J. SMITH, JR.

*Department of Chemistry and the James Franck Institute,
The University of Chicago, Chicago, Illinois*

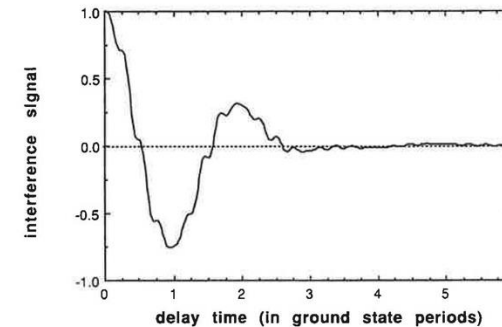
VÍCTOR ROMERO-ROCHÍN

*Instituto de Física, Universidad Nacional Autónoma de México,
México, D.F.*

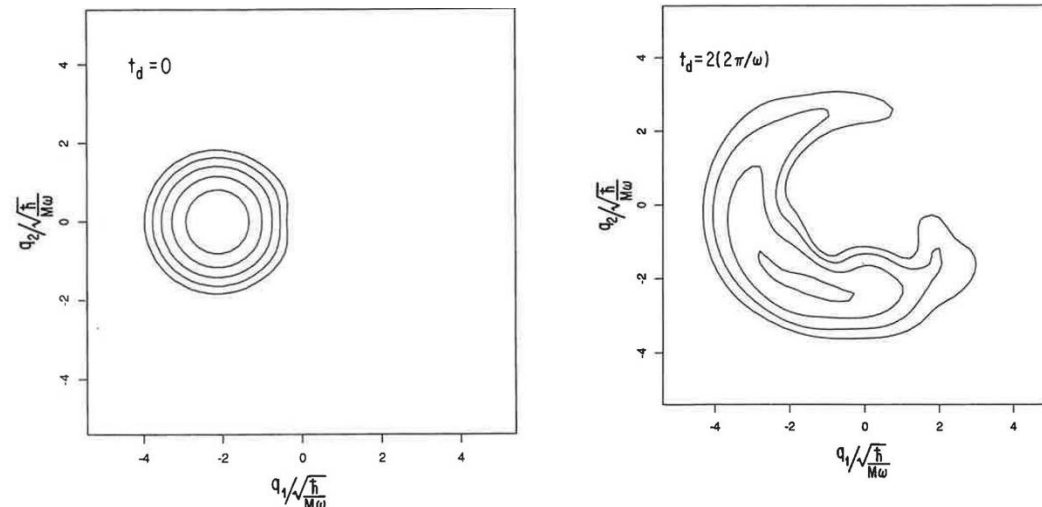
Adv. Chem. Phys (1992)

Experiment in molecules never happened
Timing challenging
Orientation of molecules in condensed phase
More complicated potentials

Example predicted experimental signal



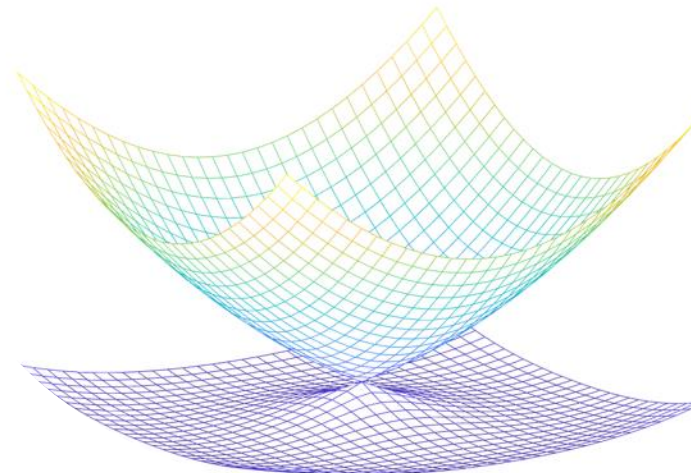
Computational view of the wave packet



Simple conical intersection

- A two-dimensional harmonic oscillator with two spin-dependent displacements.

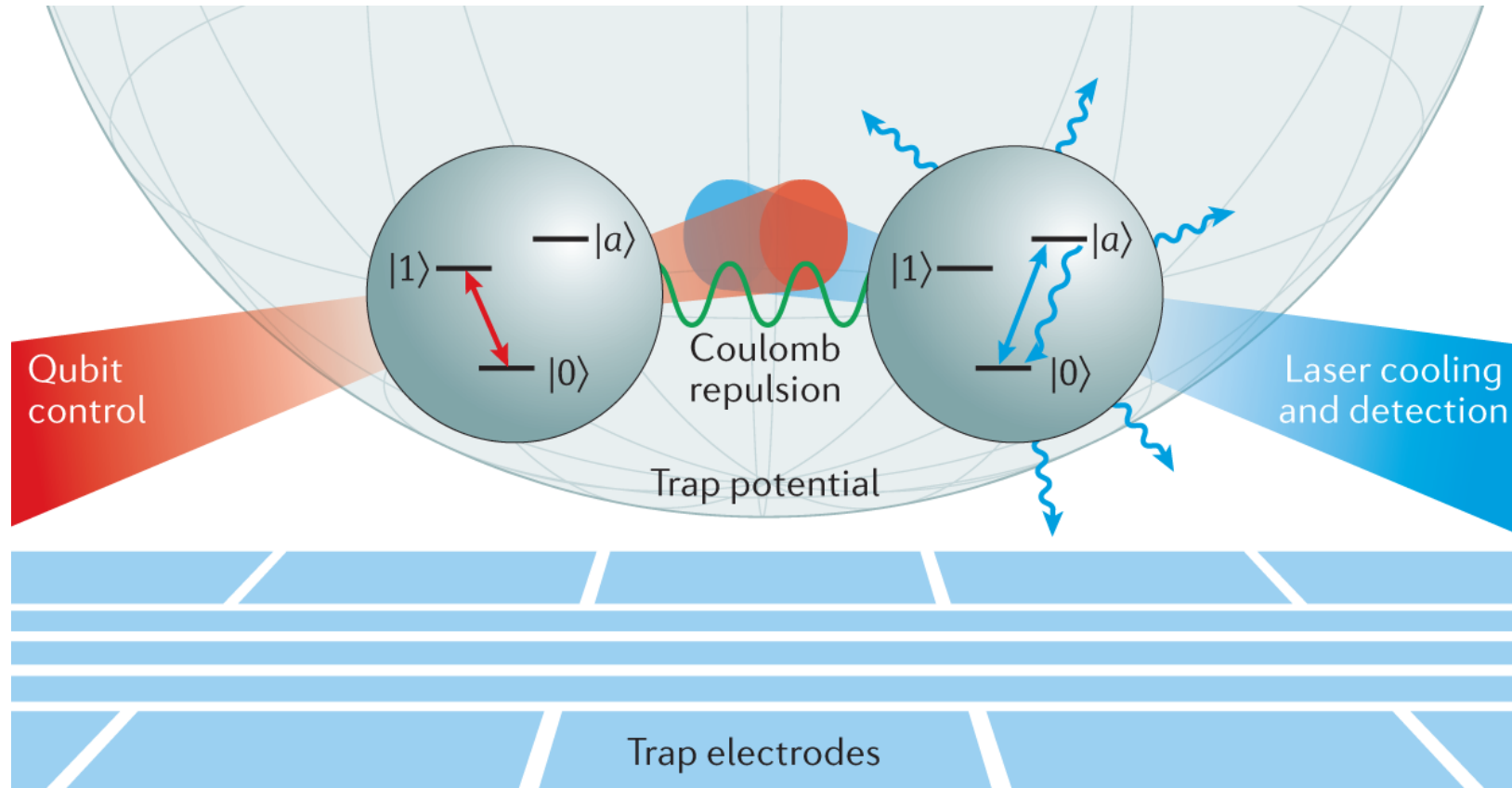
$$H = \sum_{q=\{x,y\}} \frac{p_q^2}{2m} + \frac{mq^2}{2} + F_q \sigma_q q$$



- Adiabatic potential energy surfaces where the spin is the eigenstate of $F_x \sigma_x x + F_y \sigma_y y$

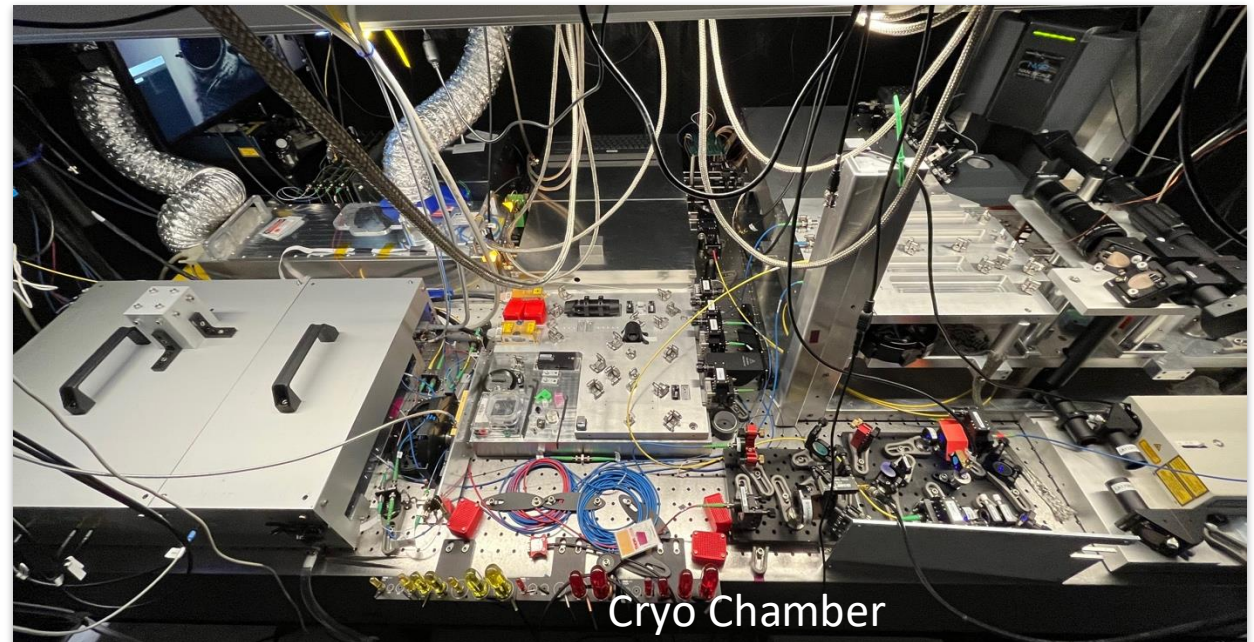
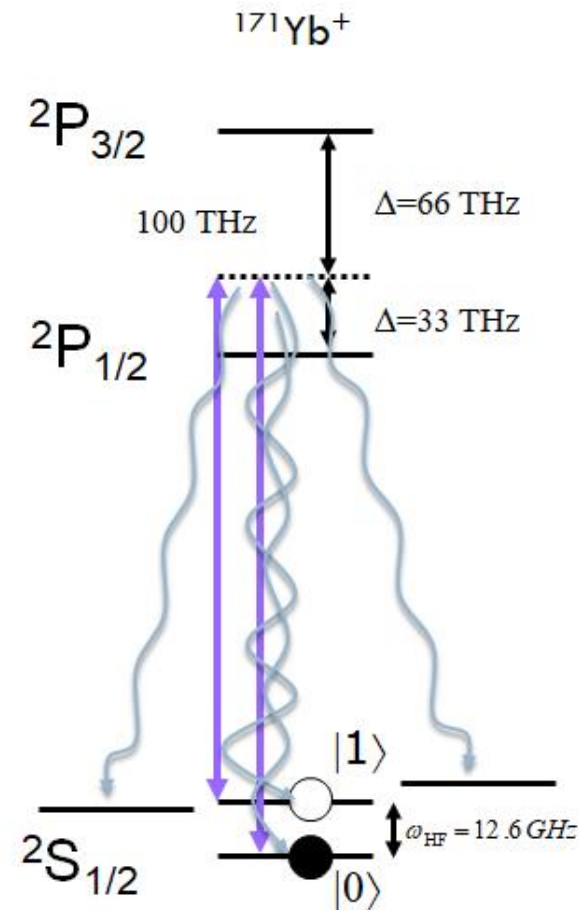
Independent approach: McDowell et al. arxiv.org/abs/2012.01852 (Kassal), Chemical Science (2021)

Controlling trapped ions

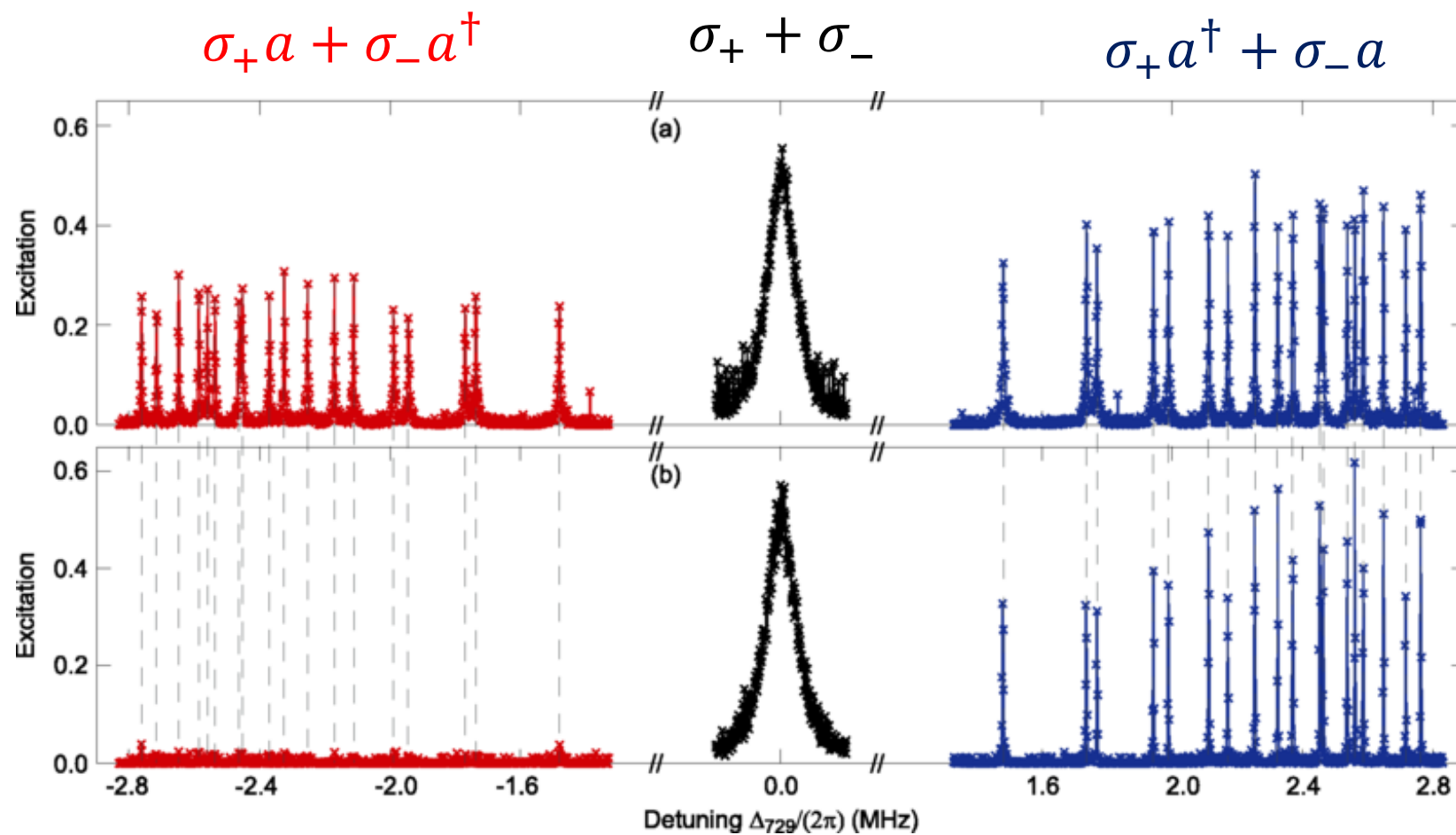


KRB, J. Chiaverini, J.M. Sage, and H. Häffner.
Nat Rev Mater 6, 892 (2021)

Gates with Raman Lasers



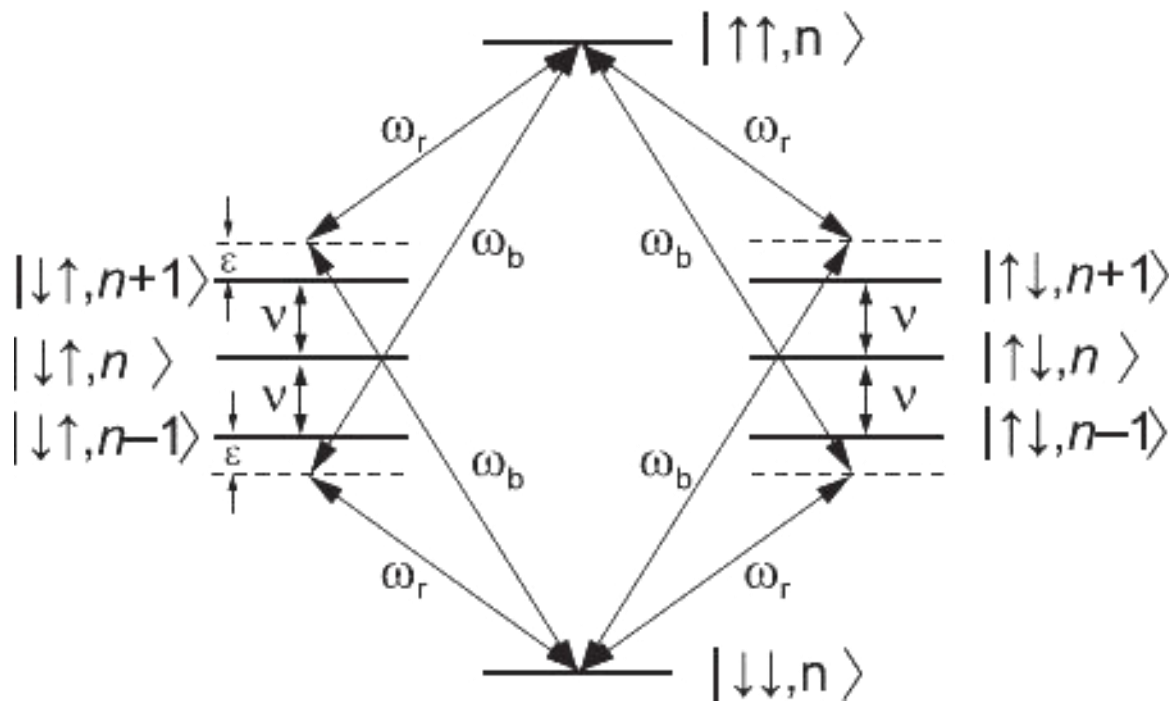
Ion and Motion



R. Lechner et al. PRA (2016)
Innsbruck

Two Qubit Pulse Sequences

Ion internal states entangled via shared motional modes



$$U = \exp(-i \theta/2 \mathbf{X} \mathbf{X})$$

A . Sorensen and K. Molmer PRL (1999)

$N = 5$ normal modes

\vec{v}_1	↑	↑	↑	↑	↑
\vec{v}_2	↑	↑	•	•	↓
\vec{v}_3	↑	•	•	•	↑
\vec{v}_4	•	↑	•	•	↓
\vec{v}_5	•	↑	•	•	•

Similar ideas: Solano and Milburn

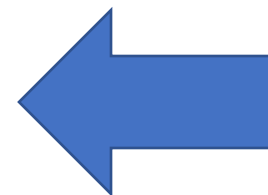
Mølmer-Sørensen gate

- Ion Trap Hamiltonian for sideband transitions:

$$H = \sum_{i,k=1}^N \frac{1}{2} \eta_{ik} \sigma_x^i \Omega_i(t) (a_k^\dagger e^{i\theta_k(t)} + a_k e^{-i\theta_k(t)})$$

$$\theta_k(t) = \int_0^t \delta_k(t') dt', \quad \delta_k(t) = \mu(t) - \omega_k$$

Hamiltonian in
interaction picture
coupling ion
internal state with
motional modes



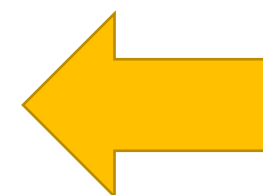
- After solving TDSE by Magnus expansion, unitary:

$$U_{MS} = \exp\left(\sum_{k=1}^N \hat{\alpha}_k(t) a_k^\dagger - \hat{\alpha}_k^\dagger(t) a_k\right) \exp(-i\beta(t) \sigma_x^i \sigma_x^j)$$

$$\hat{\alpha}_k(t) = \frac{1}{2} (\eta_{ik} \sigma_x^i + \eta_{jk} \sigma_x^j) \int_0^t \Omega(t') e^{i\theta_k(t')} dt'$$

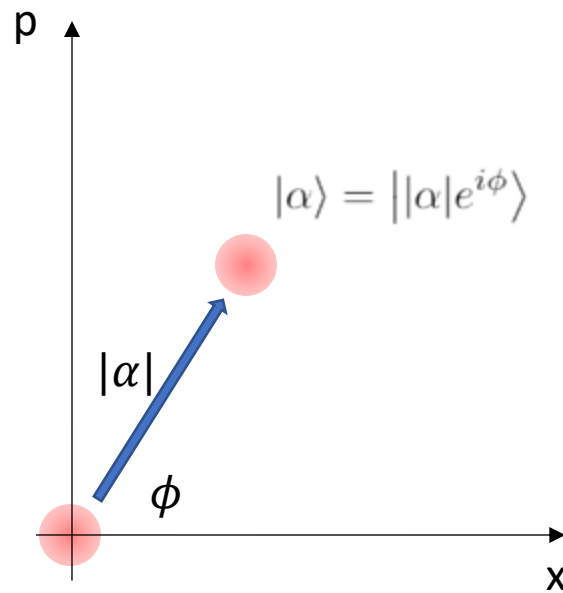
$$\beta(t) = \sum_{k=1}^N \frac{1}{2} \eta_{ik} \eta_{jk} \int_0^t \int_0^{t'} \Omega(t') \Omega(t'') \sin(\theta_k(t') - \theta_k(t'')) dt'' dt'$$

Dynamics can be
described by a
second-order
Magnus
expansion

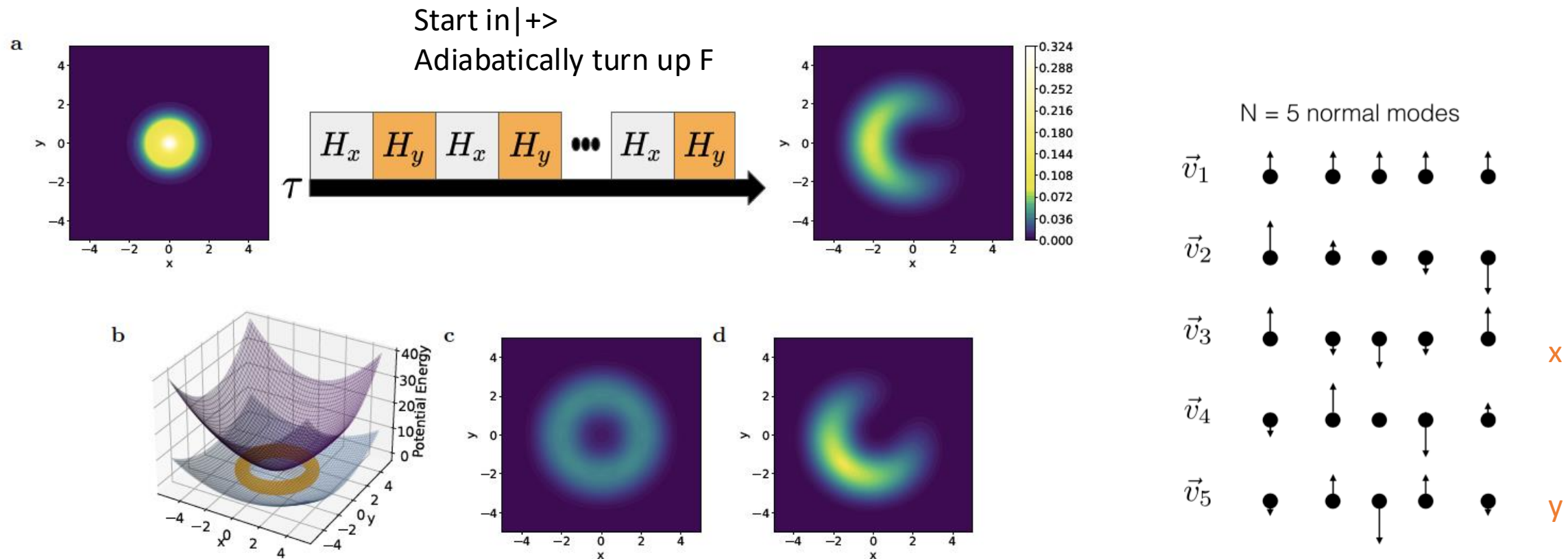


Controlling Motion Modes

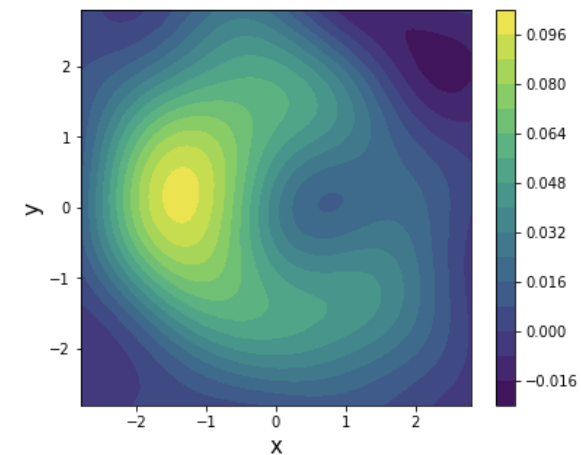
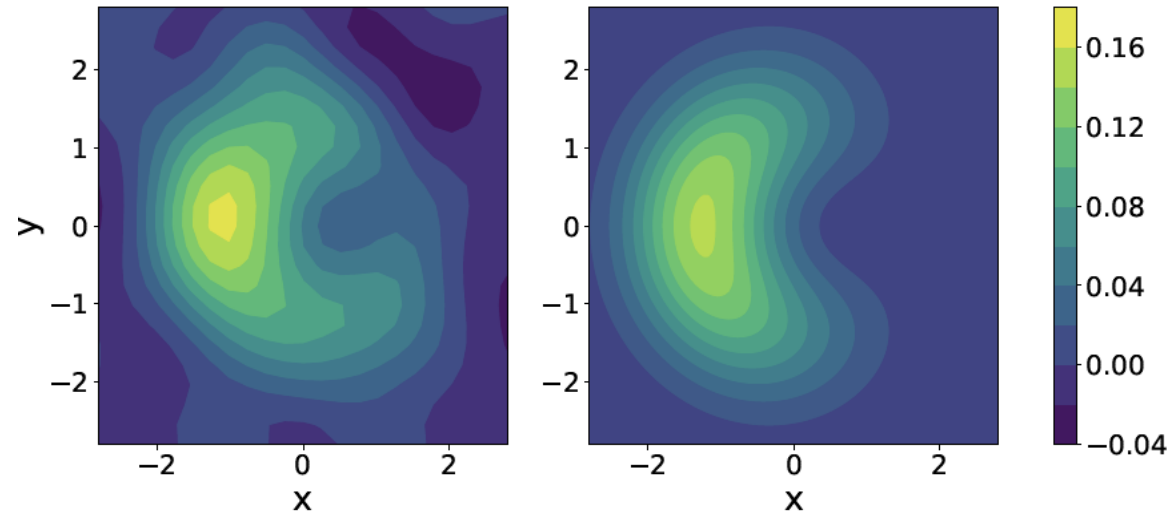
In phase space:



Experimental method and expected results

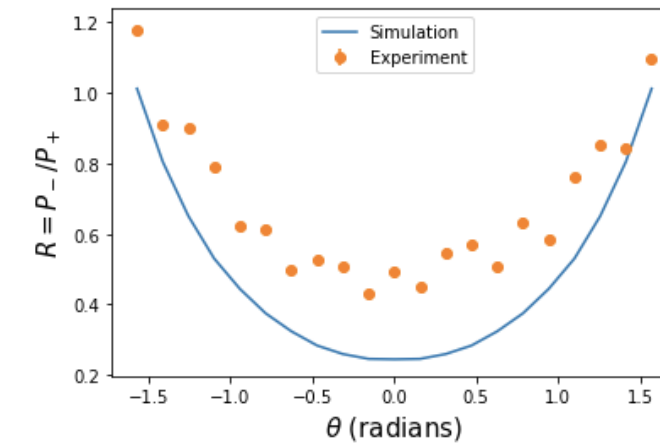
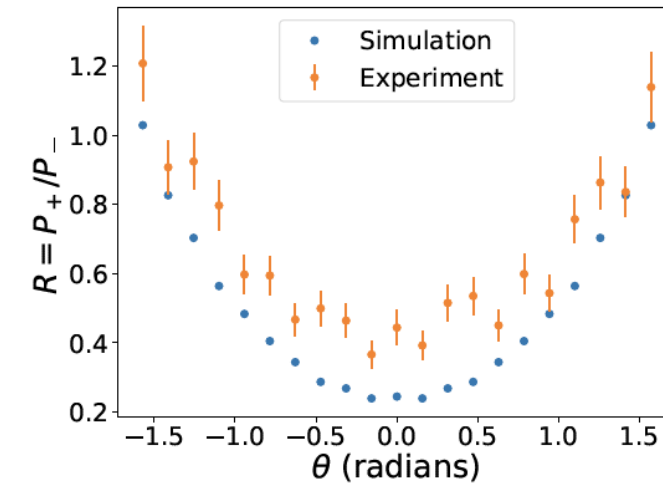


Robust feature



Whitlow et al. Nature Chem. (2023)

Similar work: Valahu et al. Nature Chem. 2023 (Kassal, Tan, Sydney)

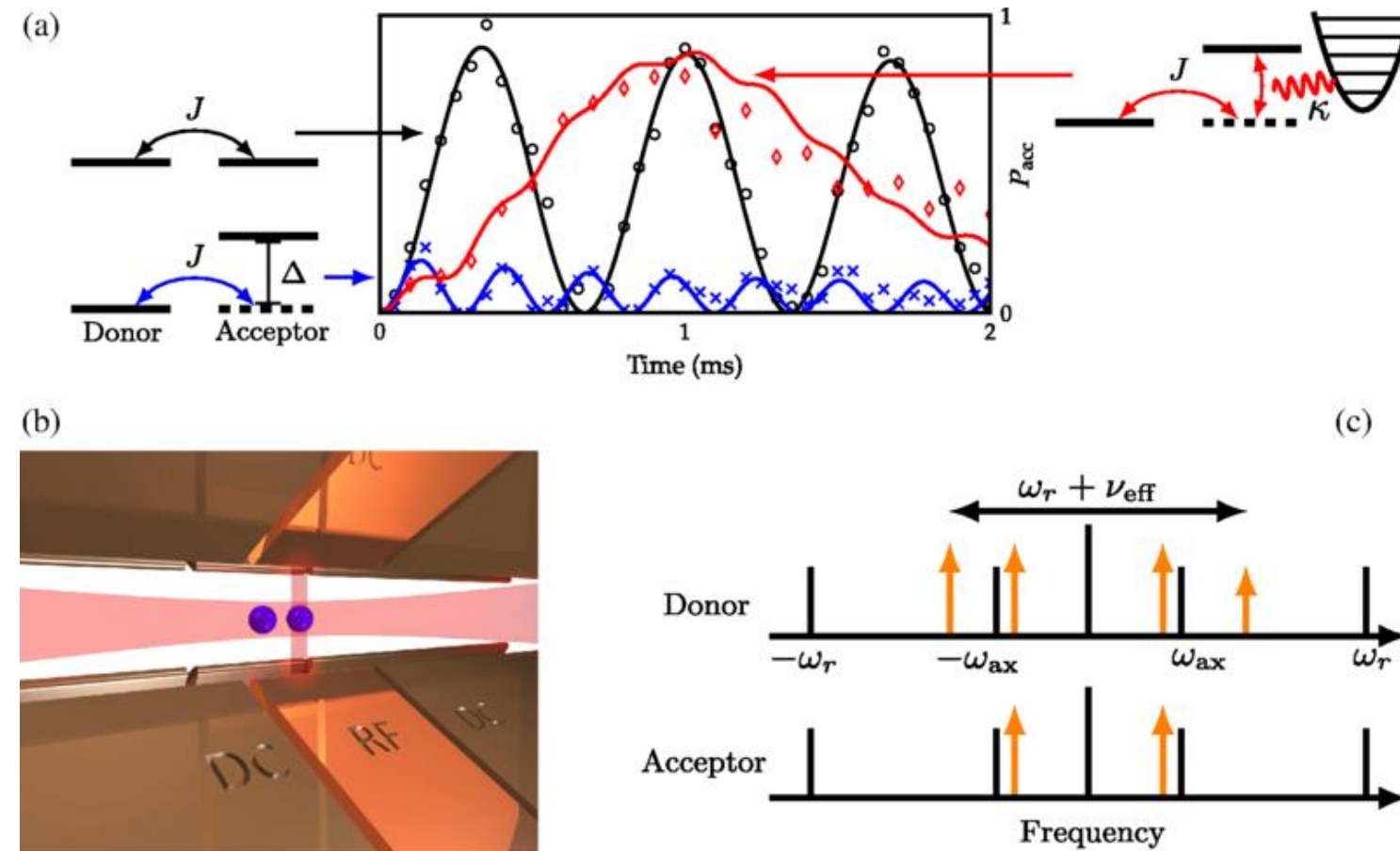


Engineering Vibrationally Assisted Energy Transfer in a Trapped-Ion Quantum Simulator

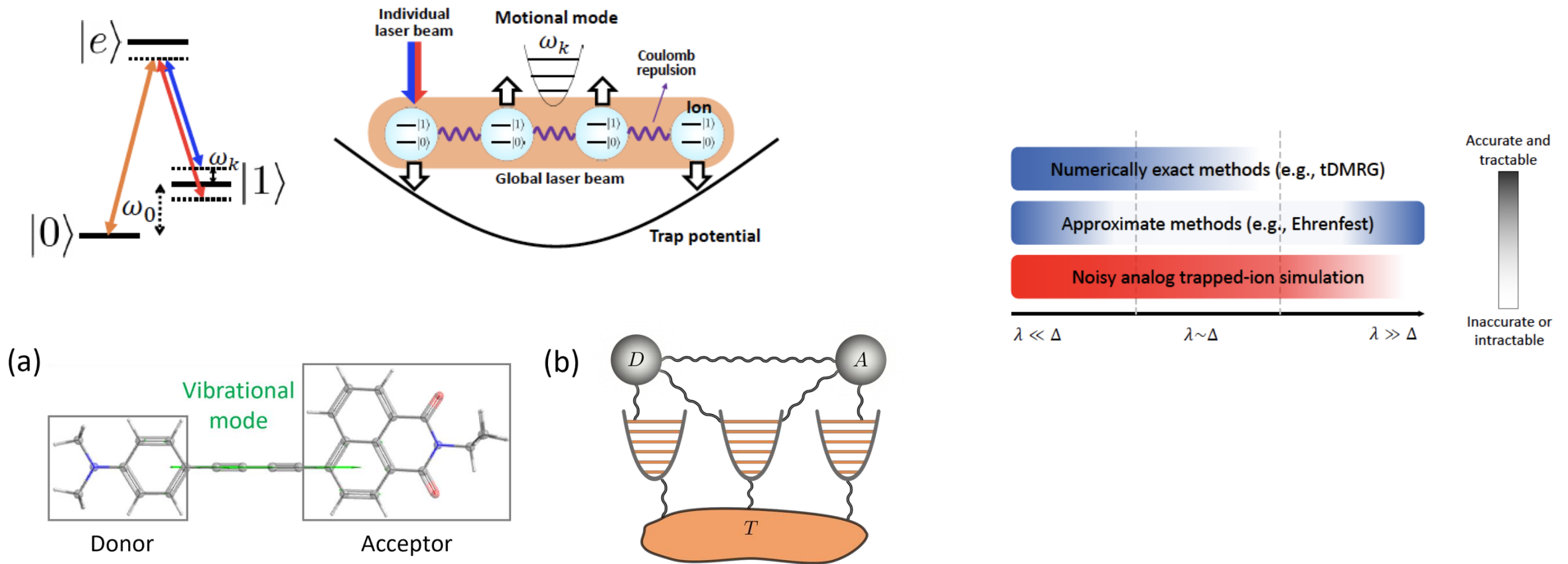
Dylan J Gorman, Boerge Hemmerling, Eli Megidish, Soenke A. Moeller, Philipp Schindler, Mohan Sarovar, and Hartmut Haeffner

Phys. Rev. X **8**, 011038 – Published 7 March 2018

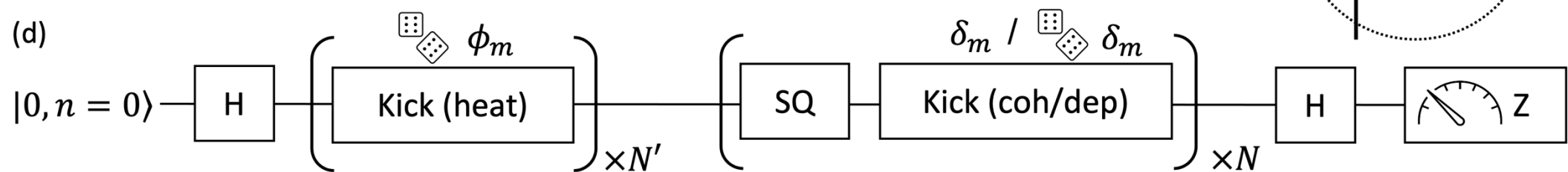
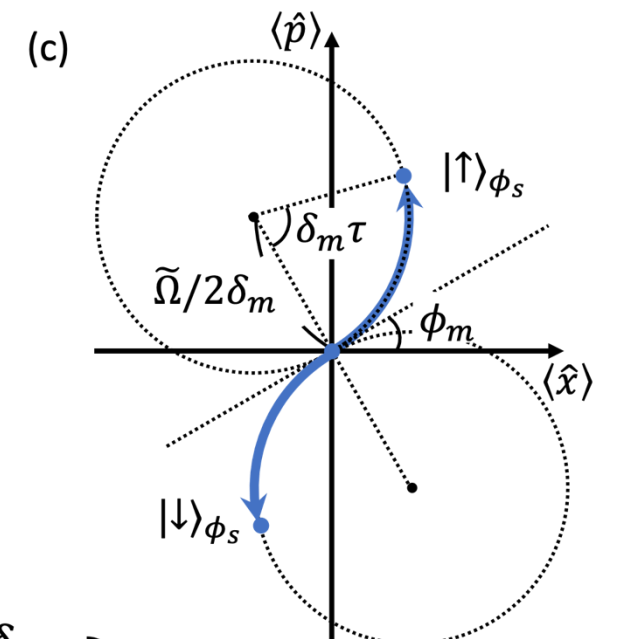
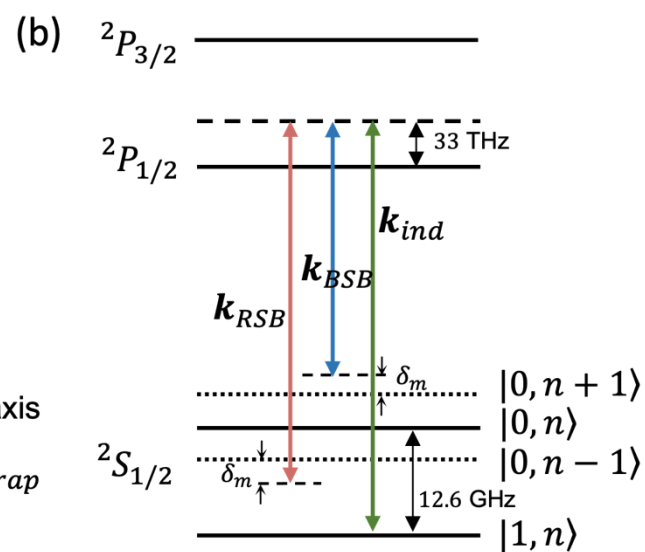
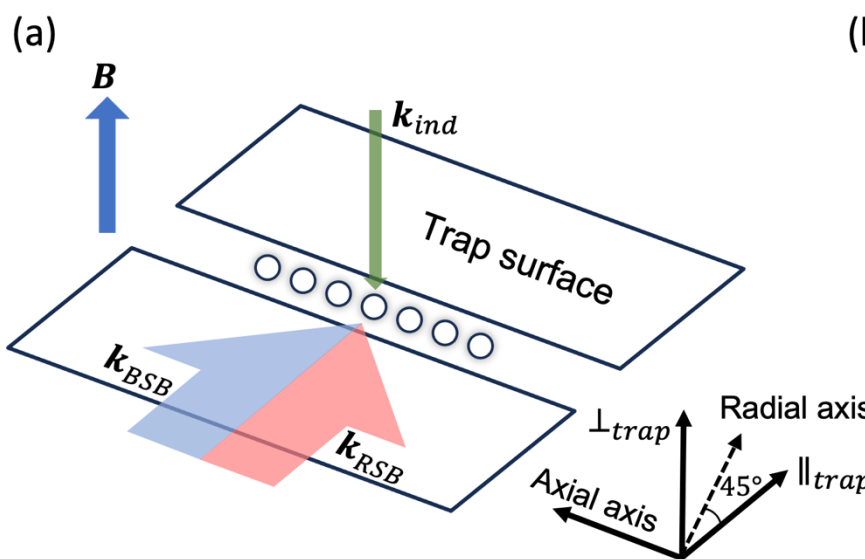
Physics See Synopsis: [Quantum Simulators Tackle Energy Transfer](#)



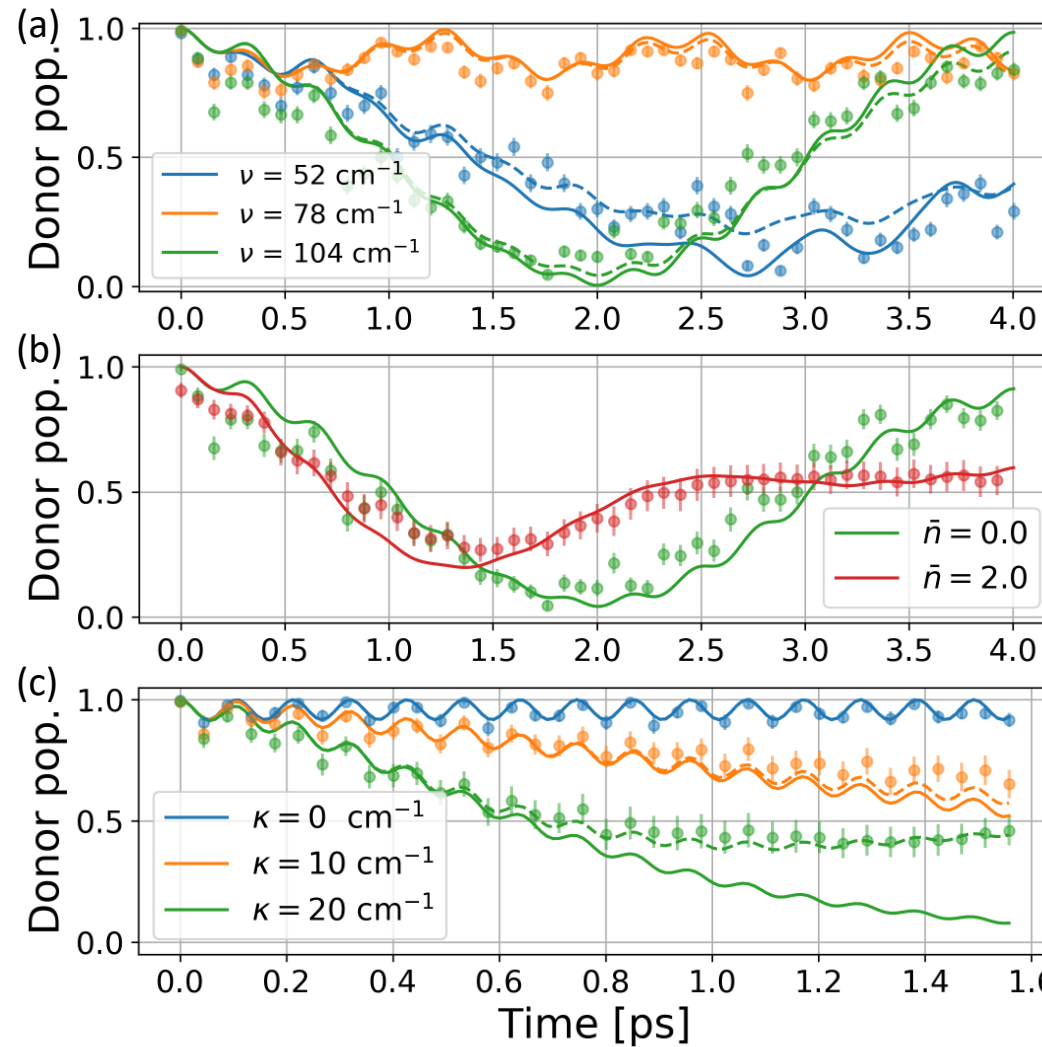
Ion Traps for Chemical Dynamics



Structured Bath



Vibrational Assisted Energy Transfer



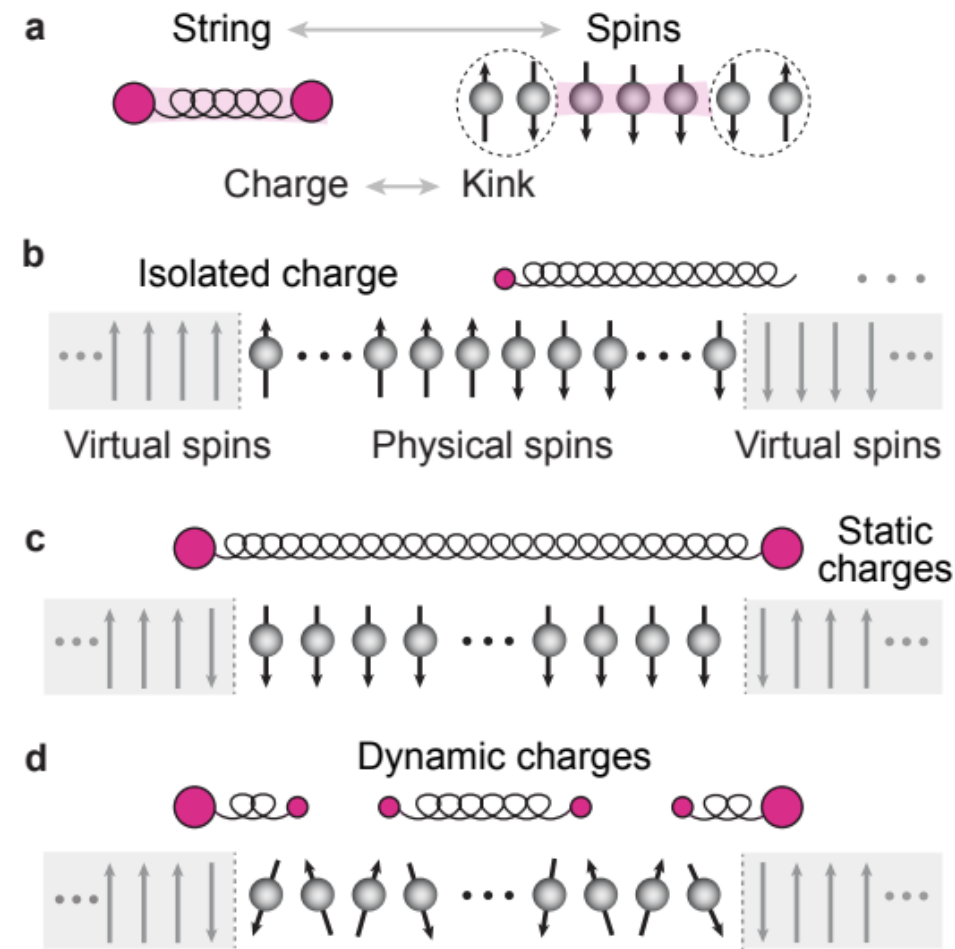
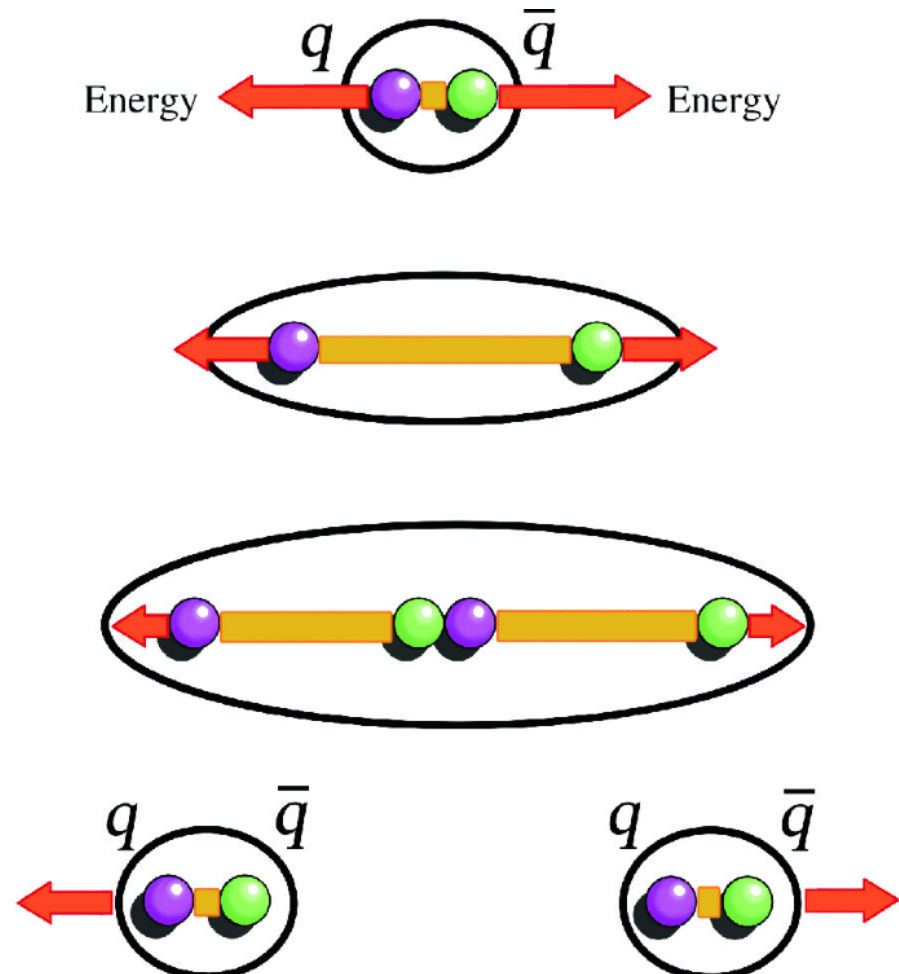
Observe resonant and harmonic enhancement

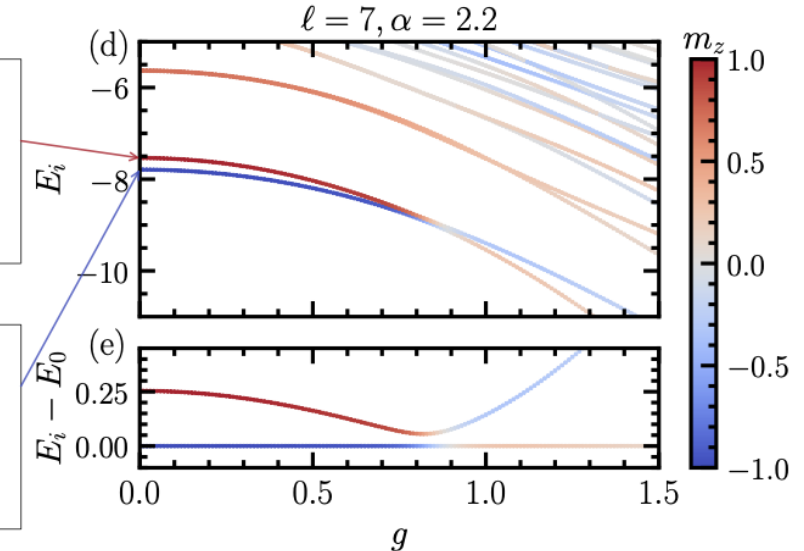
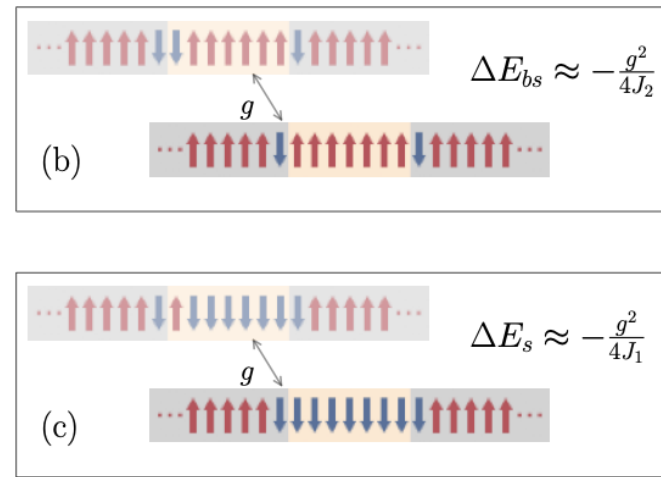
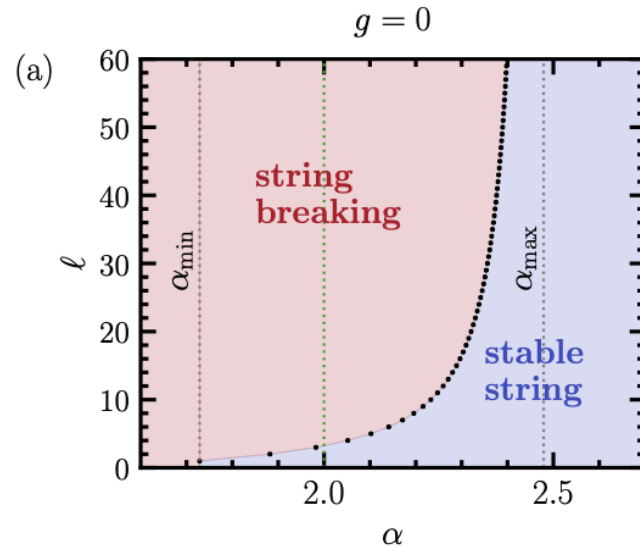
Wash out oscillations with higher temperature bath

Emulate a T_1 process with a T_2 process

Related Work with Tunable Dissipation:
V. So et al. arXiv:2405.10368 (Pagano)

High energy physics and nuclear physics



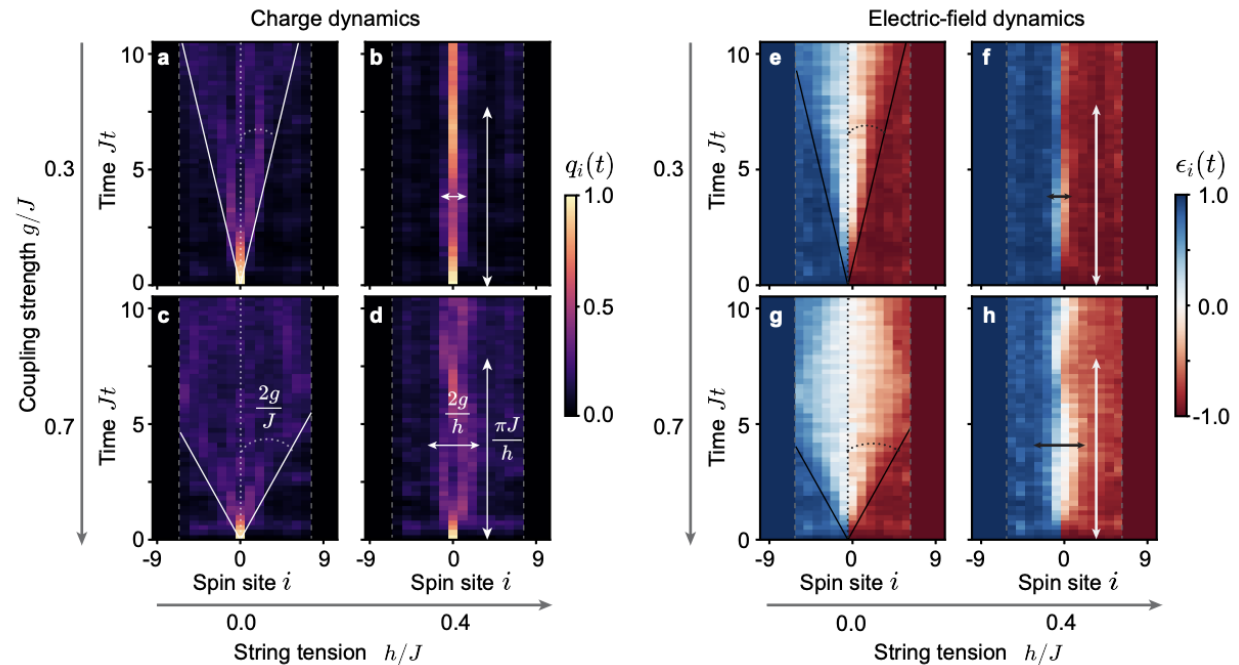


String-Breaking Dynamics in Quantum Adiabatic and Diabatic Processes

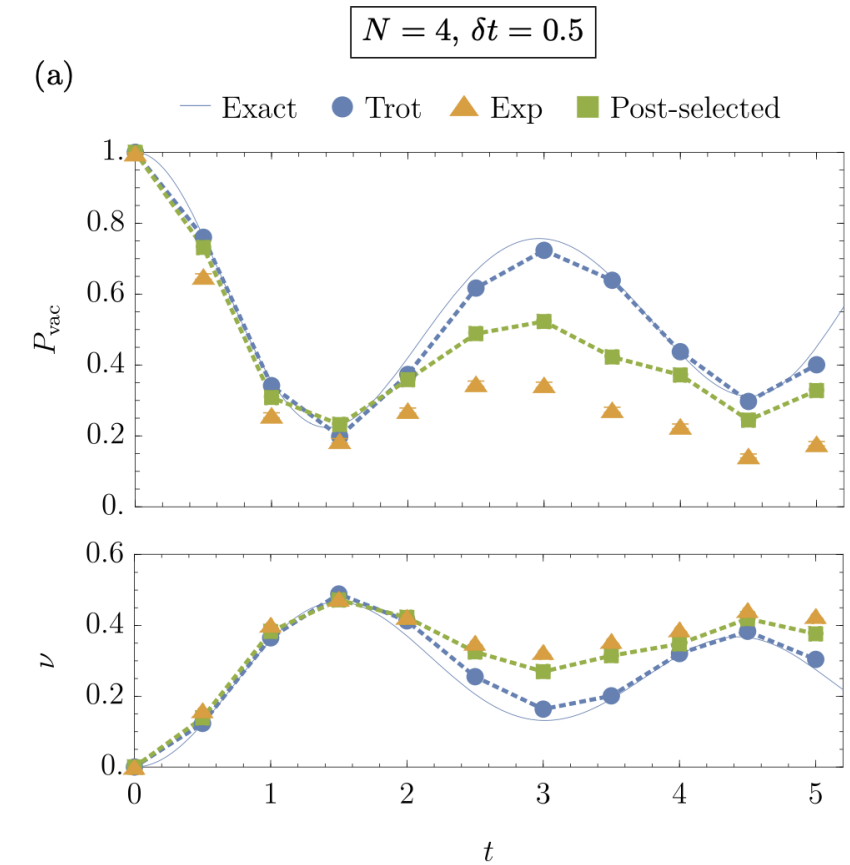
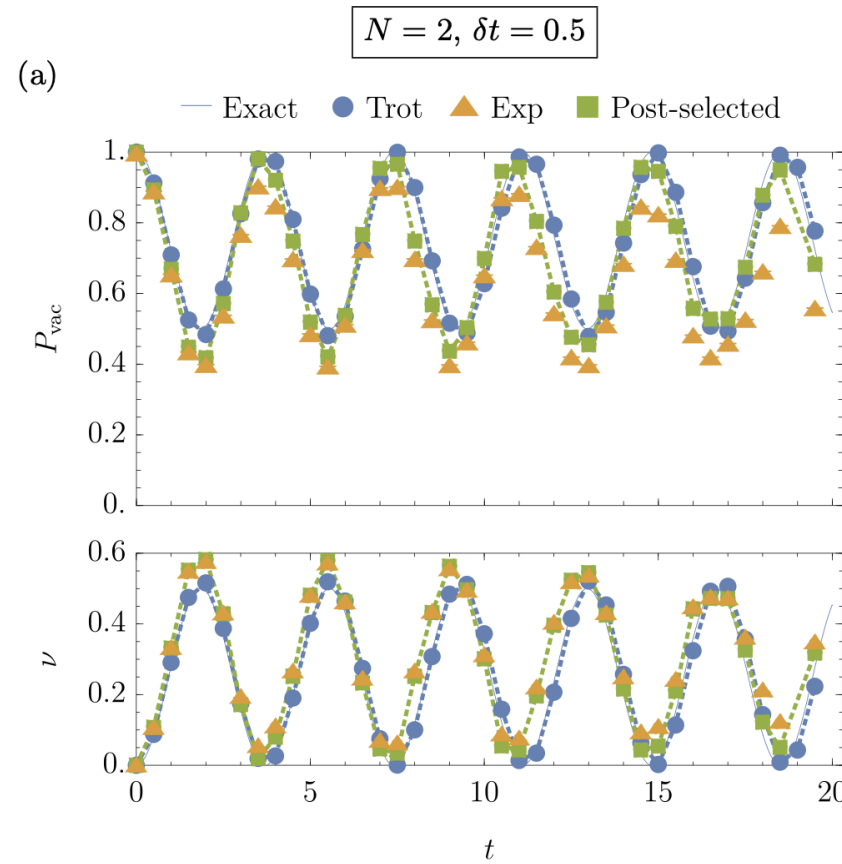
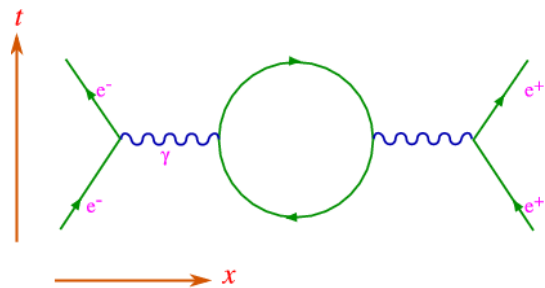
F. N. Surace et al. arXiv:2411.10652

Observation of string-breaking dynamics in a quantum simulator

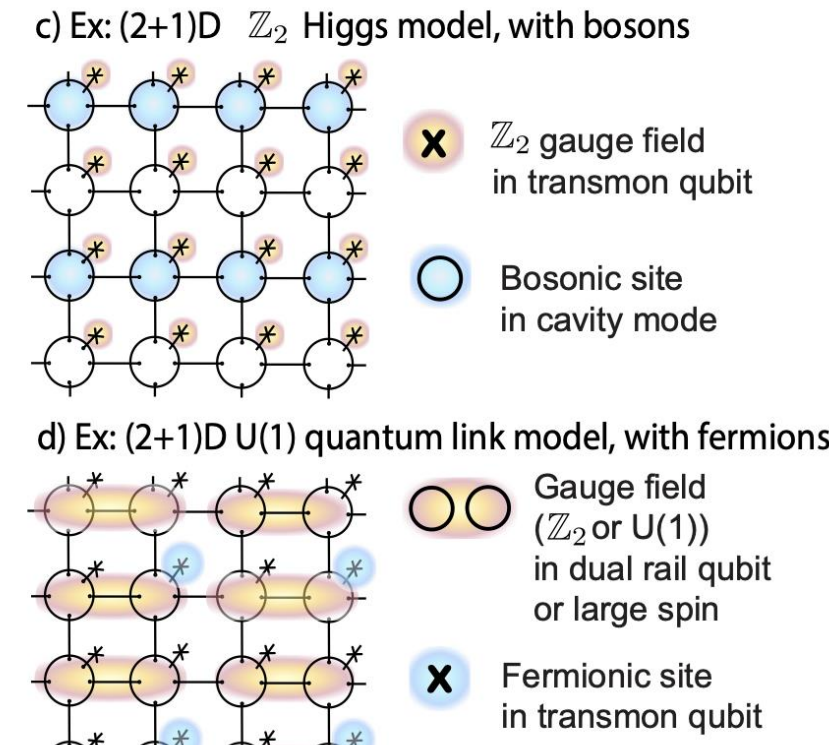
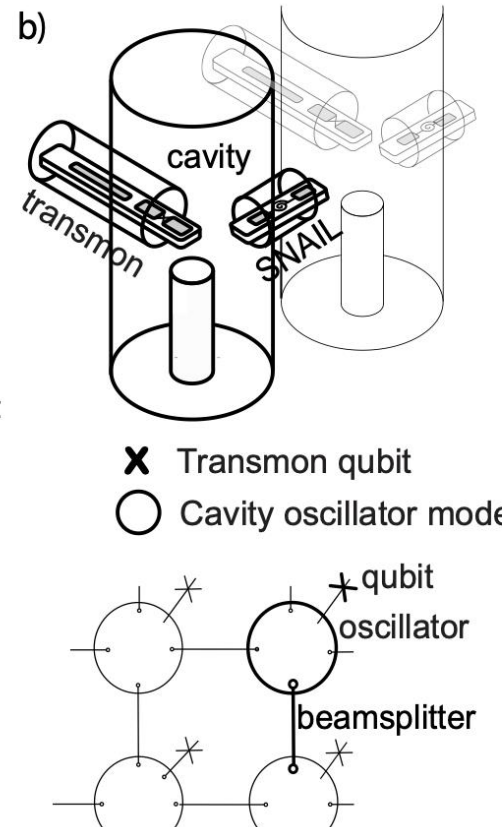
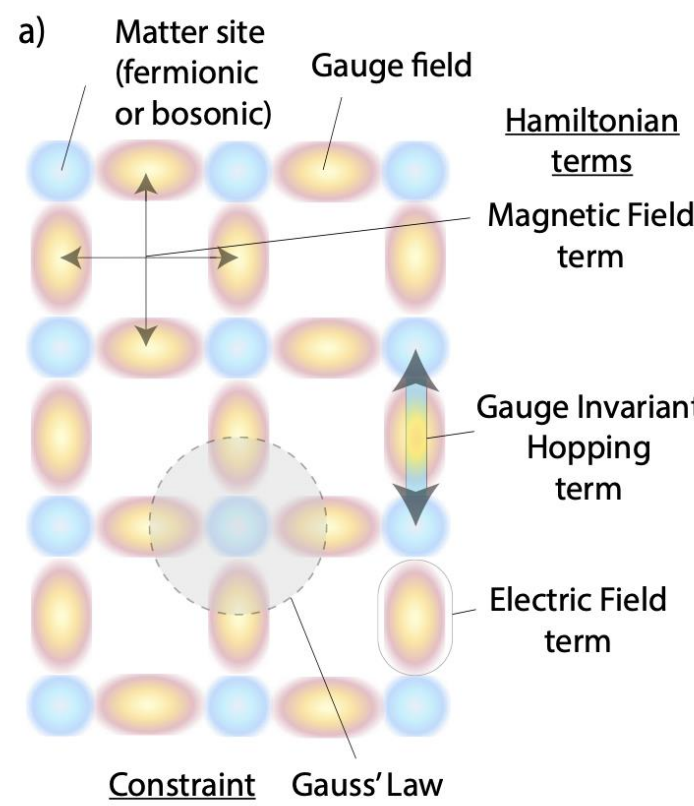
A. De et al. arXiv:2410.13815



Schwinger Model. 1+1D QED



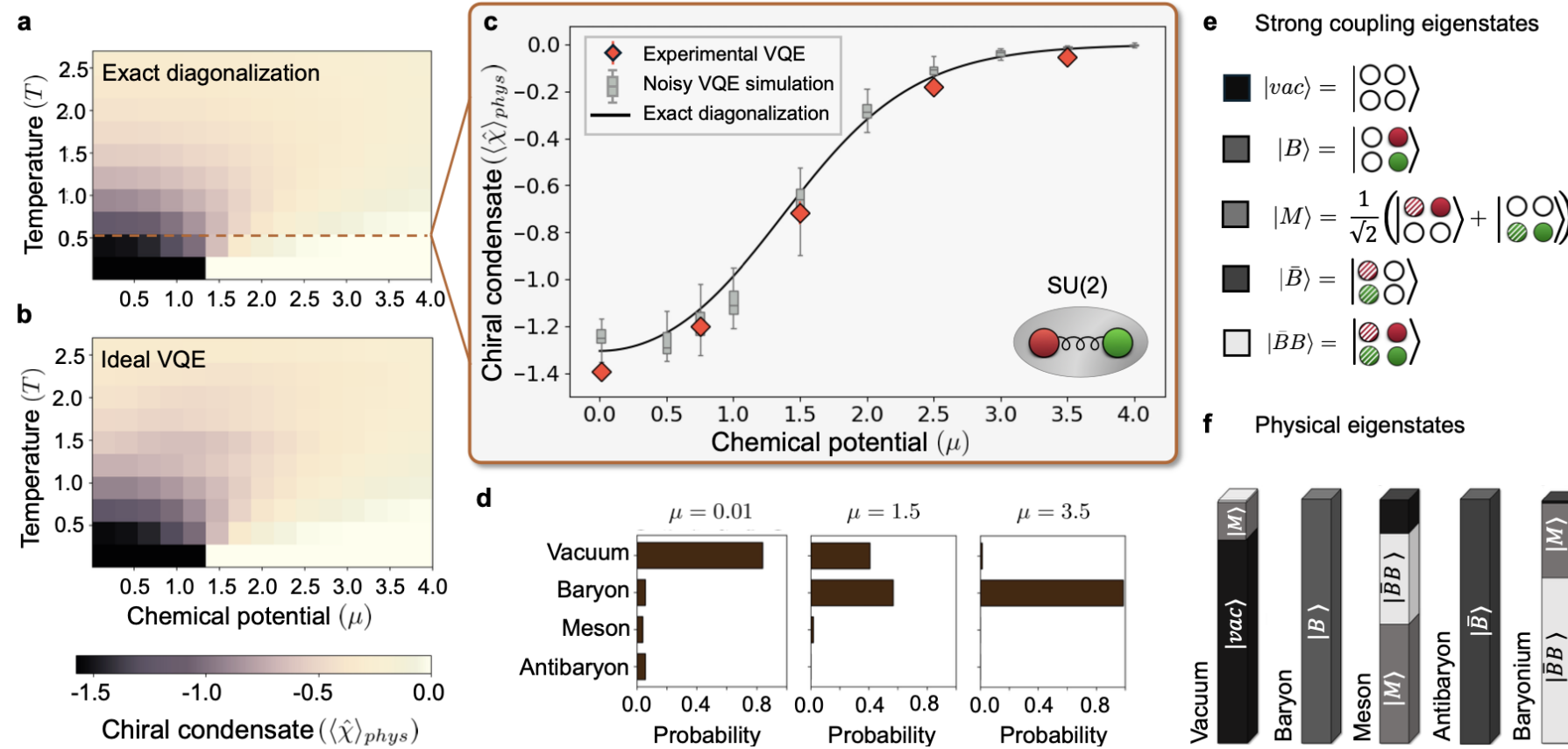
Hybrid Oscillator-Qubit Quantum Processors: Simulating Fermions, Bosons, and Gauge Fields



E. Crane et al. arXiv:2409.03747

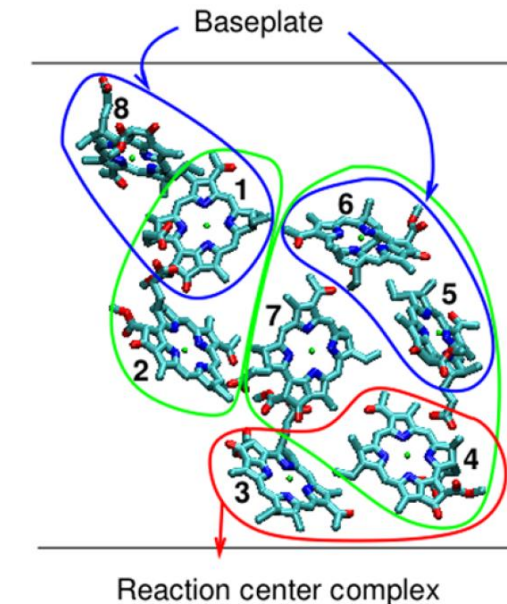
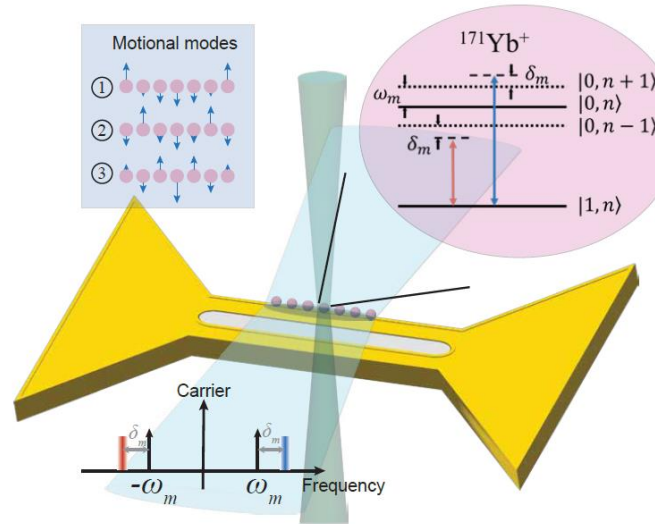
Ions: J.Y. Araz, M. Grua, J. Montgomery, F. Ringer, arXiv:2410.07436

Bosons as thermal bath



Conclusion

- Spins and bosons can be used to study chemical dynamics, nuclear physics, and particle physics
- Quantum advantage may be possible when the vibronic coupling is similar in energy scale to the electronic energy splitting
- System control allows us to include tunable dissipative effects



brownlab.pratt.duke.edu

ELD



LIGGETT & MYERS TOBACCO CO
CIGARETTE
MANUFACTURERS
FACTORY N° 42
DIST OF N.C.

Brown Lab and MIST Lab Fall 2023



Institute for
Robust Quantum
Simulation
ST1Q



QUANTUM SYSTEMS ACCELERATOR
Catalyzing the Quantum Ecosystem



Duke
PRATT SCHOOL of
ENGINEERING



Duke Quantum Center

Duke Quantum Center

Thomas Barthel

Kenneth Brown

Robert Calderbank

Marko Cetina

Di Fang

Jungsang Kim

Alex Kozhanov

Natalie Klco

Norbert Linke

Huanqian Loh

Travis Nicholson

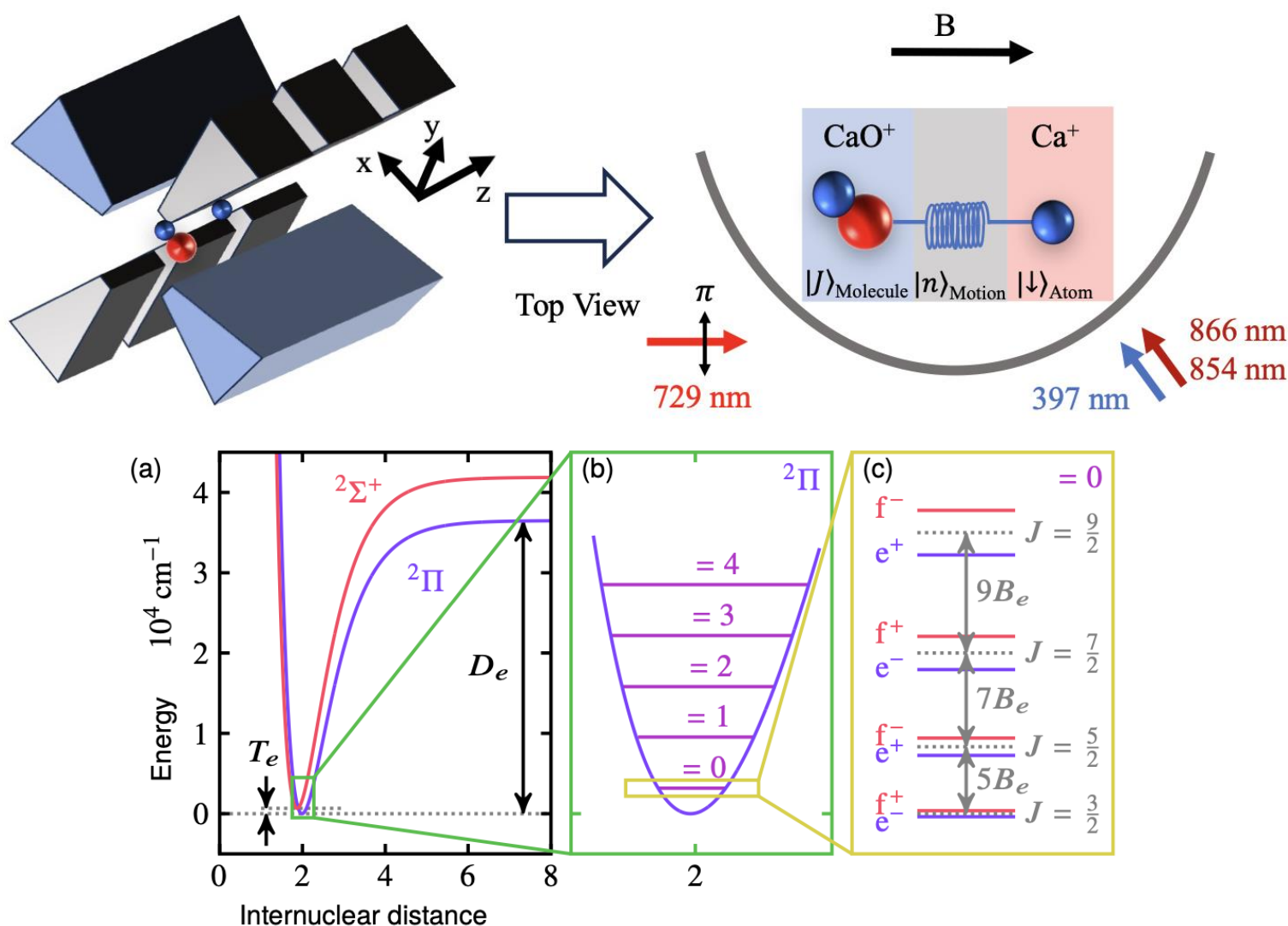
Crystal Noel

Chris Monroe

Henry Pfister

Yu Tong

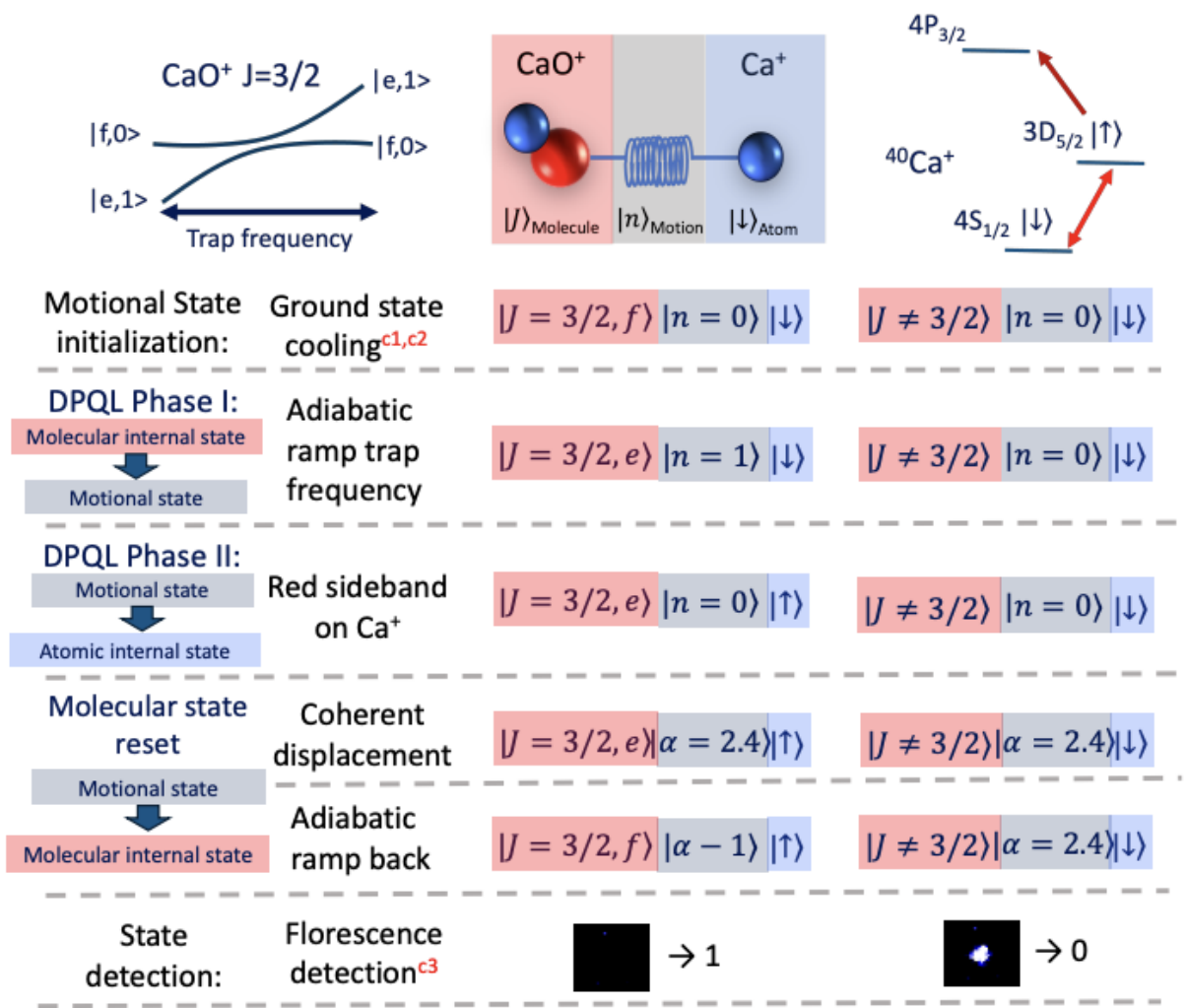




- W. Campbell and E.R. Hudson, Phys. Rev. Lett. **125**, 120501 (2020) arXiv:1909.02668
 M. Mills et al. Phys. Chem. Chem. Phys. **22**, 24964 (2020) arXiv:2008.09201
 L. Qi, E. C. Reed, B. Yu, and K. R. Brown, arXiv:2411.07137

	A_{SO} (cm $^{-1}$)	B_e (cm $^{-1}$)	ω_e (cm $^{-1}$)	D_e (eV)	PDM (Debye)	$10^{-3} \cdot T_e$ (cm $^{-1}$)	Λ-doublet splitting (MHz)				4 K/300 K Population (%)			
							$J=3/2$	$5/2$	$7/2$	$9/2$	$J=3/2$	$5/2$	$7/2$	$9/2$
BeO $^+$	-117	1.44	1242	3.8	7.5	9.4	3.8	16	42	84	89/2.1	10/3.1	1/3.9	0/4.6
MgO $^+$	-130	0.53	718	2.3	8.9	7.3	0.19	0.84	2.1	4.3	54/0.8	32/1.1	11/1.5	3/1.8
CaO $^+$	-130	0.37	634	3.3	8.7	0.7	0.45	1.9	5.0	10	42/0.5	32/0.8	17/1.0	6/1.3
SrO $^+$	-147	0.31	659	4.2	7.5	0.4	0.16	0.67	1.7	3.5	0/0.1	0/0.1	0/0.1	0/0.1
BaO $^+$	-214	0.24	506	2.2	7.9	1.5	0.089	0.39	0.98	2.0	0/0	0/0	0/0	0/0
YbO $^+$	-132	0.28	601	2.2	7.0	1.0	0.14	0.59	1.5	3.0	33/0.4	30/0.6	20/0.8	10/1.0
RaO $^+$	-228	0.20	451	3.3	7.7	0.3	0.081	0.35	0.89	1.8	25/0.3	26/0.5	21/0.6	14/0.8
BeS $^+$	-310	0.71	875	3.4	7.6	15.7	0.11	0.45	1.2	2.3	66/1.2	27/1.8	6/2.3	1/2.8
MgS $^+$	-303	0.25	469	2.0	9.2	12.9	0.0051	0.022	0.056	0.11	30/0.4	29/0.6	21/0.8	12/1.0
CaS $^+$	-299	0.15	390	4.0	11.3	5.0	0.0028	0.012	0.031	0.062	19/0.3	22/0.4	20/0.5	16/0.6
SrS $^+$	-316	0.12	423	3.1	8.7	0.3	0.0086	0.036	0.094	0.19	16/0.1	20/0.2	19/0.3	16/0.4
BaS $^+$	-273	0.08	291	3.3	9.1	2.5	0.00093	0.0040	0.010	0.021	11/0.1	14/0.2	15/0.2	15/0.3
YbS $^+$	-254	0.10	345	2.2	7.8	4.6	0.0013	0.0056	0.014	0.029	13/0.1	17/0.2	18/0.3	16/0.3
RaS $^+$	-405	0.07	266	4.5	9.4	2.7	0.00043	0.0018	0.0047	0.0094	10/0.1	13/0.1	14/0.2	14/0.2

Table 1 A list of dipole-phonon quantum logic (DPQL) candidates in electronic state $^2\Pi_{3/2}$. This table includes the spin-orbital coupling constant (A_{SO}), rotational constant (B_e), vibrational constant (ω_e), dissociation energy (D_e), permanent dipole moment (PDM), energy interval between two lowest electronic states (T_e), Λ-doublet splitting and population of several low-lying rotational states. The ground electronic state of all the species in this table is $X^2\Pi_{3/2}$, except for SrO $^+$ and BaO $^+$, whose ground state is $X^2\Sigma^+$ and the first excited state is $A^2\Pi_{3/2}$.



L. Qi, E. C. Reed, B. Yu, and K. R. Brown, arXiv:2411.07137

